

# The Response of the Hadley Circulation to Climate Changes, Past and Future

David Rind and Judith Perlwitz  
NASA/GISS at Columbia University  
New York, N.Y. 10025

## ABSTRACT

A suite of altered climate experiments for the Paleocene, the Last Glacial Maximum and a  $2\times\text{CO}_2$  climate were compared to assess the factors responsible for producing variations in Hadley Cell intensity and extent. The climate simulations used best-guess topography and marine surface fields, as well as feasible alternative SST patterns. The individual contributions to the circulations were quantified, and compared among the different simulations. The results show that the Hadley Cell intensity is associated with the gradient in latent heat release from the tropics to the subtropics, driven in the model by the gradient in sea surface temperature. It is not related to the absolute warmth of the climate, or of the tropical sea surface temperatures. Eddy forcing, primarily through transient eddy heat transport, amplified the subtropical portion of the cell, as well as the mid-latitude Ferrel Cell. The poleward extent of the Hadley Cell is affected by numerous processes, including the influence of topography in the extratropics. It also does not vary systematically with global mean temperature. Only the strongest Hadley Cell changes are longitudinally homogeneous, there is little relationship between the change in Hadley Cell intensity and the change in strength of the Walker Cell, and the Pacific Ocean is the most important basin for the zonal average Hadley Cell response. Although the latitudinal-average precipitation does respond interactively with Hadley Cell intensity and extent, the soil moisture variations are less correlated, due to differing seasonal effects and the influence of temperature/evaporation changes. The importance of the Hadley Cell variations for assessing past and future water availability changes should not be overestimated, although it is a contributing factor.

## INTRODUCTION

As the dominant zonally-averaged circulation feature at low and subtropical latitudes, the Hadley Cell represents an organizing principle in which to understand locations of climatological features, such as deserts and rainforests. In the current climate, the distribution of deserts in the descending zone of the Hadley Cell at a wide range of longitudes is evidence of its applicability. This then is a lure for viewing paleoclimate and future climate in the same context; how did/will the Hadley Cell change, with its implications for past/future water availability, vegetation etc.

How are we to understand and compare the climate-induced changes in the various forcing functions influencing the Hadley Cell? The regions of large-scale meridional and vertical motion that characterize this circulation feature respond to the governing principles of conservation of energy and momentum. Starting from these equations, we can derive the applicable terms. These can be written with respect to the mass streamfunction  $\psi$ . In addition to the definitions given below, the various terms used in equations (1) and (2) are given in an appendix at the end of the article.

Define (1)  $\bar{v} = -\frac{\partial \bar{\psi}}{\partial p}$   $\bar{\omega} = \frac{\partial \bar{\psi}}{\partial y}$ ; as  $\frac{\partial \bar{v}}{\partial y} + \frac{\partial \bar{\omega}}{\partial p} = 0$ ,  $-\frac{\partial^2 \bar{\psi}}{\partial y \partial p} + \frac{\partial^2 \bar{\psi}}{\partial y \partial p} = 0$

From the zonally-averaged equations of motion, we can derive:

$$(2) \frac{\partial^2 \bar{\psi}}{\partial y^2} + \frac{f^2}{S_p} \frac{\partial^2 \bar{\psi}}{\partial p^2} = \nabla^2 \bar{\psi} = \underbrace{\frac{-f}{S_p} \frac{\partial}{\partial p} \left( \frac{\partial \bar{u}}{\partial t} + \bar{v} \frac{\partial \bar{u}}{\partial y} + \bar{\omega} \frac{\partial \bar{u}}{\partial p} \right)}_{\text{NONLINEAR MOMENTUM FLUX}} + \underbrace{\frac{1}{S_p} \frac{\partial}{\partial y} \left( \frac{\partial \bar{T}}{\partial t} + \bar{v} \frac{\partial \bar{T}}{\partial y} \right)}_{\text{NONLINEAR THERMAL FLUX}} - \underbrace{\frac{f}{S_p} \frac{\partial \bar{L}}{\partial p} - \frac{f}{S_p} \frac{\partial \bar{F}_x}{\partial p}}_{\text{MOMENTUM FORCING}} - \underbrace{\frac{1}{S_p c_p} \frac{\partial \bar{Q}}{\partial y} + \frac{1}{S_p} \frac{\partial \bar{G}}{\partial y}}_{\text{THERMAL FORCING}}$$

where friction F includes surface friction, mountain torque and cumulus friction, and heating Q includes short and longwave radiation, latent heat release, convective motions, and sensible heat flux.

The eddy forcing terms are

$$(3) \quad \bar{G} \equiv \frac{\partial(\bar{v}'T')}{\partial y} + \frac{\partial(\bar{\omega}'T')}{\partial p} \quad \text{eddy heat flux divergence}$$

$$\bar{L} \equiv \frac{\partial(\bar{u}'v')}{\partial y} + \frac{\partial(\bar{u}'\omega')}{\partial p} \quad \text{eddy momentum flux divergence}$$

The Laplacian of the streamfunction that appears on the left-hand side of equation (2) is negatively related to the streamfunction, assuming a sinusoidal relationship. So the various terms on the right-hand side force a negative value of  $\bar{\psi}$ . With the streamfunction defined as above, the Hadley circulation in December-February is characterized by a negative value of the streamfunction, and positive values of the forcing terms as written intensify the Hadley Cell.

Which terms are dominant for Hadley Cell intensity and extent? Various researchers have emphasized different components, often in simple models in which the other terms are minimized. For example, Schneider and Lindzen (1977) emphasized the

importance of cumulus heating and cumulus friction in driving the intensity of the axisymmetric circulation, while Becker and Schmitz (2001) (for stationary eddies), Trenberth and Stepaniak (2003) (for transient eddies) and Kim and Lee (2001) emphasized the importance of eddy fluxes in driving the Hadley Cell. Lindzen and Hou (1988) calculated that the intensity of the circulation increased dramatically as heating moves off the equator, and hence is dominated by near-equatorial displacements of the thermal equator, while Fang and Tung (1999) noted that the time-dependent solution does not show this dominance as clearly, and the results of Dima and Wallace (2003), using reanalysis data, support the view that the seasonal variations are instead driven by the monsoons.

Considering the latitudinal or poleward extent, Held and Hou (1980) emphasized the importance of the latitudinal temperature gradient and tropopause height (in a model assuming conservation of angular momentum in the Hadley Cell regime, and no eddy forcing at mid-latitudes), while, Taylor (1980), for example, emphasized the importance of eddy momentum transports. As noted by Kim and Lee (2000) one difficulty is that these sources are not independent of one another; eddies are associated with latent heat release that influences  $dQ/dy$  and surface friction affecting  $dF/dp$ , as well as heat and momentum transport convergences ( $dG/dy$ ,  $dL/dp$ ). The results in the individual calculations also appear to be sensitive to the various parameters used, including the thermal relaxation time (Fang and Tung 1997) or the effective viscosity (Kim and Lee, 2001).

Pfeiffer (1981) used radiosonde data and estimated atmospheric heating profiles to calculate some of the budget terms shown in Equation (2). Comparing the relative importance of eddies and diabatic heating for the current climate, he concluded that eddy fluxes of heat and momentum were responsible for 1/3 to 1/4 of the total Hadley circulation intensity, and the latitudinal extent (from his figures) was the result of both eddy forcing and the diabatic circulation. This conclusion is hindered by the approximate nature and sparse sampling of the data.

General circulation model studies obviously include all of these terms together, but they can be varied systematically to study the relationships amongst them. Rind and Rossow (1984) performed such experiments, and discussed the complex interactions between the various thermal and momentum forcing terms that arose in the model. For example, solar forcing during Northern Hemisphere winter actually weakened the Hadley Cell intensity, for it provided out-of-phase forcing with gradients in latent heat release associated with low latitude sea surface temperature gradients (driven ultimately by solar heating in the previous seasons). Removing the frictional forcing terms from the model completely destroyed the Hadley circulation even without altering solar radiative forcing. Experiments in such models emphasize the need to incorporate as many terms as possible, even those which from scale-analysis would seem to be secondary; they may decide the outcome of competition between the larger forces, and are especially important when the ageostrophic flow field is being considered.

The GISS GCM has also been used to evaluate the dependence of the Hadley Cell on systematically varied sea surface temperature gradients in warmer and colder climates (Rind, 1998; 2000). An increased (decreased) gradient led to an intensified (weakened) Hadley Circulation independent of any change in global mean temperature; the warmer climate by itself actually led to a small decrease in Hadley Cell intensity. The latitudinal

gradient did not affect the width of the Hadley circulation. We return to these results in the discussion section.

Finally, GCM studies of other climates have been compared to assess how the Hadley Cell changes with climate. In transient future warming experiments (IPCC 2001), tropical precipitation increases, especially over the oceans, with some decreases in the subtropics, implying an increased Hadley Cell intensity. In  $2\times\text{CO}_2$  experiments there is little consistency; Rind et al. (2001a) found that even within the GISS suite of models, there were both increases and decreases in Hadley circulation intensity. In ice age experiments, much depends on the magnitude of tropical cooling, a question of considerable uncertainty (e.g., Rind and Peteet, 1985). We compare the results given below with other model simulations in the discussion section, in an effort to assess their generalizability.

Given the potential importance of various forcing terms, and the inconsistency in models, we need to determine how the individual components change in a wide range of climate simulations. That is the focus of this paper.

## II. MODEL SIMULATIONS

In contrast to some of our other studies in which one variable was changed at a time, here we look at a range of modeled paleo/future climate simulations in which many aspects of the climate are different. The sea surface temperatures are uncertain for these periods, especially in the tropics, therefore, each simulation is accompanied by an alternate with a different, plausible sea surface temperature pattern. All the simulations are done with the GISS Global Climate/Middle Atmosphere model (GISS GCMAM), which extends up to the mesosphere, at  $8^\circ\times 10^\circ$  resolution. The reason for including the full stratosphere is to allow the effect of gravity wave drag parameterizations to be apparent; separate sensitivity experiments are used to illustrate this effect on the Hadley Cell via the momentum budget. The effect of the coarse resolution and model physics is discussed by reference to higher resolution runs which were performed for several of these climate simulations. Each of the simulations discussed here has been published previously, albeit without particular emphasis on its Hadley Cell response.

How accurately does this model simulate the observed Hadley Cell and its variability? To address this question, we ran the model with the observed sea surface temperatures for the time period 1950 through 1997. Results are shown in Figure 1, giving the stream function values and their variability. A negative value represents a clockwise mass flux circulation in the frame of the figure, hence the Dec-Feb Hadley Cell, whereas a positive value gives the opposite circulation sense, i.e., the June-Aug Hadley Cell. The control run simulation (top panels) has a magnitude about 10-20% weaker than in the NCEP analysis [which differs somewhat from the ECMWF analysis (Trenberth et al. 2000)], and also a weaker Ferrel Cell, likely due to its coarse resolution. For a similar reason, the poleward extent is about  $10^\circ$  poleward of its observed position. The model's transient eddy energy is about 85% of the observed value, while its standing eddy energy is actually greater than observed (the coarse resolution results in waves moving too slowly). What is important for the budget terms however, are the eddy heat and momentum transports and their convergences. Hansen et al. (1983) show a comparison of the coarse grid model transports with observations; while the magnitude of both the heat and momentum transports by eddies is appropriate, the momentum transport peaks

around 10° poleward of the observed peak, altering the eddy forcing of the Ferrel Cell.

The model's variability for the two solstice seasons is shown in the middle panels. Peak values are on the order of 10% of the seasonal mean. The monthly standard deviations, with the seasonal cycle removed, and the difference between 7 El Niño and La Niña time periods are shown in the bottom figures. These can be compared with results given by Waliser et al. (1999) from NCEP/NCAR reanalysis data. The reanalysis results showed maximum variability near the equator of some  $15 \times 10^9 \text{ kg s}^{-1}$  in excellent agreement with the model values; the chief discrepancy is that the observed variability ("5" contour) extended further poleward into the extratropics. The reanalysis data also showed a streamfunction difference between El Niño and La Nina conditions of about  $10 \times 10^9 \text{ kgs}^{-1}$  in both hemispheres, again in agreement with model values. Note that variability estimated using in situ radiosonde observations (Oort and Yienger, 1996) produces larger magnitude patterns off the equator, which appear to be due to undersampling of the Pacific Ocean region (Waliser et al., 1999).

The primary simulations used in this study are shown in Table 1, along with the reference that provides greater details on the simulation. In addition to the present climate control run, they include simulations for the Paleocene (58 million years ago), characterized by very low topography and a reduced latitudinal temperature gradient, with extensive high latitude warming; for the Last Glacial Maximum (21k BP), with increased topography due to ice sheets, and an increased latitudinal temperature gradient; and for the doubled CO<sub>2</sub> climate. The standard simulations for the Paleocene and Last Glacial Maximum include the "best guess" sea surface temperature (SST) patterns for those periods, while the alternate simulations include prescriptions that provide more of a tropical response, consistent with some data or model studies (see the noted references). Two additional ice age runs were also performed that have reduced topographic gravity wave drag, as is discussed below. The standard doubled CO<sub>2</sub> simulation with the GISS model has a large tropical response, and the alternate, similar to that originally performed with the Geophysical Fluid Dynamics Laboratory (GFDL) model, has less tropical and more high latitude warming.

Some characteristics of these simulations are provided in Table 2, and the changes in Dec-Feb sea surface temperatures from the control run are shown for the different experiments in Figure 2. The warmer conditions in the tropics and high latitudes for the doubled CO<sub>2</sub> and the Paleocene are clearly visible, with much the reverse conditions for the Ice Age runs. Also evident is the difference between the standard and alternate simulations, especially in the tropics. In this and several of the following figures we show the run with the relatively warmer sea surface temperatures for each climate in the left hand column (hence PAL-A is shown on the lower left).

The zonally-averaged surface air temperature changes for the solstice seasons are given in Figure 3. The global surface air temperature range of these simulations is some 17°C, the global topography differs by up to 280m, and the equator-to-pole surface air temperature gradient changes by 30°C. The Paleocene simulations also have somewhat different land-ocean distribution, with a smaller Atlantic Ocean and no ice sheets on Antarctica (thus the large warming in that region in June-Aug). These simulations represent an extremely wide range of conditions to test hypotheses concerning Hadley Cell variations.

All experiments are run with the specified sea surface temperatures/sea ice, obtained either through paleodata analysis or model simulations. The runs are for 20 years following a spin-up year; with the specified ocean conditions the simulations are stable throughout the course of the integration. The differences among the experiments are evaluated for their significance from the interannual variability in the control run.

### III RESULTS

The changes in the streamfunction for the two solstice seasons are given in Figure 4(a,b), with the significance of the change indicated by the shading. Light (dark) shading means a significant increase at the 95% level in the negative (positive) value of the streamfunction, hence an increase in Dec-Feb (June-Aug) Hadley Cell value.

It can be seen from these presentations that the Hadley Cell changes involve alterations in both the peak magnitude and latitudinal/altitude distribution. The percentage change in the peak value is listed in Table 2, with the significant changes indicated in bold face (for the 20 year simulations in these extreme climates, for seasonal averages, all the peak changes are significant, as are most of the changes shown in Figure 4; all the temperature and energy changes in Table 2 are highly significant).

The results show that across the suite of experiments the Hadley Cell intensity is not simply related to global or equatorial temperatures. In Dec-Feb, the Hadley Cell was strongest in the Paleocene and weakest in 2CO<sub>2</sub>-A despite their similar tropical SST magnitudes; in June-Aug, the Hadley Cell was strongest in Ice Age-A and weakest in Paleocene-A despite the Ice Age tropical SSTs being some 13°C colder. Hence, in the Southern Hemisphere for these particular experiments, the intensity is actually inversely related to tropical SSTs.

Also given in the table is the change in poleward extent, which we produce by linearly interpolating the vertically-integrated streamfunction value between latitudes; the Hadley Cell ends where the streamfunction changes sign. When this technique was used with an 8°x10° average of results from our 2x2.5° model, it produced generally similar latitudinal changes to those defined at the finer resolution. Nevertheless, it is at best only a crude approximation. The interannual variation of this value from the control run is 1.33° latitude for Dec-Feb, and 2.04° latitude for June-August. The significant changes are again shown in bold face in Table 2, and are in effect also indicated in Figure 3 by significant changes in the poleward extension of the streamfunction.

Again, there is little relationship between the warmth of the climate and the poleward extent of the circulation. The Hadley Cell has its greatest poleward expansion in the coldest (ice age) climate, and is most contracted in one of the warmest climates (PALEOCENE). To understand these results, we refer to the budget terms.

We calculate the contributions of the different terms proportional to the negative of the streamfunction, given in the equation (2) above. While these are generated in association with the streamfunction and its changes, to some extent they represent “forcing terms”, as commented on further in the Discussion section. The results are shown for the control run solstice seasons in Figures 5a and b (in units of Wm<sup>-2</sup> normalized by the static stability). They are divided into the contribution associated with the latitudinal gradient in diabatic heating ( $dQ/dy$ ), the mixing of momentum by convection (cumulus friction), the total eddy forcing (G+L), and the nonlinear momentum and heat flux terms which act once the circulation is set up. On the bottom is shown the

contribution from the various surface forcings that act in the lower atmosphere due to sensible heat flux, surface friction and mountain torque.

As shown in the figure, a negative value helps generate a clockwise circulation in the frame of the figure, thereby enhancing the Hadley Cell during Dec-Feb, while a positive value enhances the Hadley Cell during June-Aug (or the Ferrel Cell in Northern Hemisphere winter). In the model, the Hadley Cell is forced at low latitudes primarily by the diabatic circulation, in the subtropics by eddy forcing, cumulus friction, and surface friction/mountain torque at low levels, while the nonlinear terms amplify the circulation in the upper and lower troposphere. The mid-latitude Ferrel Cell is forced primarily by eddies, with a contribution due to the nonlinear flux, and surface friction. Compared to the selected results shown in Pfeffer (1981), the model's diabatic heating term is properly positioned but somewhat weaker, and the eddy contribution to the Hadley Cell is somewhat greater and located further poleward ; the eddy contribution to the Ferrel Cell is properly positioned but too weak. The latter effect is likely due to the coarse model resolution, while the other discrepancies may be a mixture of model inaccuracies and sampling/heating estimate uncertainties in the observations.

Each of these forcing terms was calculated for the different model simulations noted above. The change in the diabatic heating source for June-August is shown in Figure 6, along with the control run value for reference. Comparison with Figure 4b indicates a general correspondence between the variation of this term and the peak low latitude intensity in the different runs. The change in the total eddy forcing (the sum of the eddy contributions to the momentum and thermal forcing as given in the introduction) is depicted in Figure 7 for Dec-Feb. Comparison with Figure 4a (and table 2) indicates that this term is important for the subtropical Hadley Cell strength (along with the diabatic heat source).

Shown in Figures 8 and 9 are the contributions of the different terms in the runs with the biggest Hadley Cell increases, the Paleocene during Dec-Feb and the alternate Ice Age simulation during June-August (Table 2). The dominance of the diabatic heating source change is evident in these figures, along with the subtropical/mid-latitude eddy forcing changes. In addition, the surface forcing terms can be quite important at specific latitudes.

What produced these responses? We correlated the intensity and poleward extent changes in these 7 simulations (6 experiments plus control) with various aspects of the modeled climate. The results are given in Table 3. A significant response (indicated in bold) requires a correlation greater than 0.7. With respect to the general idea that a warmer climate has increased Hadley Cell intensity, the model simulations show no such effect; what correlations do exist are if anything the reverse. However, the Hadley Cell intensity is strongly correlated with the sea surface temperature gradient - with a stronger gradient from low latitudes to the subtropics, the intensity increases. The correlation is almost as high with the precipitation gradient, the latent heat release being a prime component of the diabatic heating term. This effect is less important in the Southern Hemisphere, as monsoon precipitation over land at higher northern latitudes also influences Hadley Cell intensity. Even here the relationship is strong at times; in June-August, the large Hadley Cell change in IA-A is associated with a 68% increase in the SST gradient between 27°N and 27°S, and in PAL, the change south of the equator is related to a 40% increase in the SST gradient between 4°S and 27S, while the decrease north of the equator is due to an

SST gradient reduction between 27N and 4N. There is no significant correlation between Hadley Cell intensities in the two hemispheres for their respective solstice seasons, nor between the intensity and poleward extent.

The poleward extent is inversely proportional to the precipitation gradient, since when the subsidence previously in the subtropics moves poleward, it allows for more subtropical precipitation. The poleward extent is highly correlated between the two hemispheres, but it is not simply related to either the SST gradient or eddy kinetic energy. Held and Hou (1980) calculated that the latitudinal extent should be related to the equator to pole temperature gradient, all else (e.g., the height of the tropopause) being assumed equal. A general correspondence can be seen in that the poleward extent and gradient decrease in the doubled CO<sub>2</sub> climate, and increase in the ice age climate, although the latitudinal change is not closely related to the magnitude of the gradient (e.g., 2CO<sub>2</sub>-A has greater contraction than 2CO<sub>2</sub>, although its latitudinal gradient decrease is smaller). It does not hold for the Paleocene simulations, or IA in June-August. The theory relates only to the symmetric circulation driven in the absence of mid-latitude eddies, and assumes conservation of angular momentum at low latitudes (i.e., no cumulus friction), both at variance with the model simulations and real world.

An example of the influence of momentum forcing on the poleward extent is given by the correlation with gravity wave drag in the Northern Hemisphere. The increased ice sheet topography at upper mid-latitudes in the Last Glacial Maximum runs also gave rise to increased parameterized mountain wave drag in the lower stratosphere. This parameterization is a function of the roughness (standard deviation) of the topography. Since that is not well known for the big ice sheets (e.g., Laurentide) the ice age experiments were run in two different ways. The standard simulations assume that this standard deviation is similar to that of current day ice sheets of equivalent height (even though those ice sheets, on Greenland and Antarctica, are in regions of actual mountains); this provided a large increase in mountain wave drag. Alternatively, they were assumed to be plateau-like, and thus relatively smooth, with little increase in mountain drag.

The difference in results between these two formulations is shown in Figure 10 for both the standard and alternate ice age sea surface temperature simulations. Fig. 10 (top left) shows the change during Dec-Feb of the gravity wave drag between the rough and smooth simulations, with much larger reduction of momentum in the lower stratosphere in both cases of rough topography. Since the model attempts to conserve angular momentum, there is a corresponding increase in angular momentum input by the surface friction at the corresponding extratropical latitudes (Fig.10, top right). Fig. 10 (bottom left) gives the sea level pressure differences responsible for this surface friction change. In order for the angular momentum to be increased by surface friction, there have to be relatively greater east winds at the surface, produced by having higher pressure to the north, and lower pressure to the south, as occurred. The vertical motion field change that would produce this pressure response consists of subsidence at higher latitudes and rising air at lower latitudes. This more direct circulation is illustrated by the vertically-integrated streamfunction change (Fig. 10, bottom right), with the more negative values poleward of 40°N implying an extension of the Hadley Cell direct circulation to much higher latitude.

## IV. DISCUSSION

### *A. The importance of sea surface temperature gradient—model dependency*

The model experiments over this wide range of paleo/future climates show no simple relationship between the Hadley Cell intensity and the global or equatorial temperature magnitudes, responding instead to the latitudinal temperature gradient from the tropics through the subtropics. Some theories of this region of the globe assume that the gradient is negligible, perhaps minimized by radiation feedback (e.g., Pierrehumbert, 1995). The so-called “weak temperature gradient” approximation has been proposed as a balance model for the tropics (Sobel and Bretherton, 2000), and Polvani and Sobel (2002) utilize it while calculating the Hadley Cell response to heating. Although this gradient is smaller than that across mid-latitudes, it still controls the model's precipitation gradient, and thus to a good extent the heating gradient, involving interactive feedbacks with the vertical motion field, convection and Hadley Cell intensity.

The effect is so strong that the Hadley Cell differences between the alternate SST depictions for the individual climates often exceed the differences between the different climate regimes. Similarly, the change in one solstice season bears little relationship to the change in the other, given how the gradients can differ seasonally. During Northern Hemisphere summer, the temperature (and precipitation) response over the subtropical land areas also affects the intensity, lowering the correlations with SST gradients (and emphasizing the importance of monsoon circulations for that season, as in Dima and Wallace, 2003).

It is not the latitudinal gradient *per se* that is driving the Hadley circulation, but the precipitation feedback response to the induced circulation. To the extent that the analyses by Schneider and Lindzen (1977) and Schneider (1977) using an axisymmetric model are relevant, the latitudinal gradient itself initially drives a weak low-level circulation via sensible heating. The convective feedback with latent heat release, and to some extent cumulus friction, amplifies the gradient effects and the circulation in both intensity and depth. Schneider (1977) calculated that the low level circulation driven by the gradient was sufficient to provide for enough moisture convergence to generate a significant ITCZ.

How general are these results? In idealized experiments performed with a finer resolution (and newer) version of the GISS GCM, sea surface temperature gradients were increased/decreased in a linear fashion as a function of latitude without altering the mean temperature, and also warmed/cooled while maintaining the same (altered) temperature gradient (Rind, 1998). The January and July Hadley Cell intensities were then compared. Qualitatively similar to the results shown here, in that study, with the increased gradient in January, the Hadley Cell increased by 15%; with the decreased gradient, it decreased by 12%. Simply warming the climate decreased the intensity by about 9% (with either gradient). In July the sensitivities were reduced: +3% for the increased gradient, -1% for the decreased gradient, and  $\pm 10\%$  with warming. As in the results shown here, the July situation is further complicated by the upward motion generated in the Northern Subtropics due to heating over land. The poleward extent was basically unaffected by the latitudinal gradient change, but it was increased by a few degrees of latitude in the warmer climate, an effect which is apparently overridden by the other changes in the warm/cold experiments presented here.

The magnitude of the Hadley Cell response to SST gradients does appear to be model-dependent. In several recent publications (Rind et al, 2001a, 2002a) we have noted that the sensitivity of a model to sea surface temperature variations varies with its control run characteristics. If the model's boundary layer scheme does not easily transfer these surface changes into the free atmosphere, perhaps due to weak surface winds, and if the convection scheme does not translate lower atmosphere changes into the middle and upper troposphere, perhaps due to reduced mass fluxes or lack of penetrating convection, the atmospheric results including the Hadley circulation can be much less sensitive to sea surface temperature variations. With respect to all these features, the model used for these experiments appears to be quite sensitive, although as indicated in the discussion of Figure 1, its sensitivity to SST variations is similar to that in the NCEP/NCAR reanalysis data.

In particular, the same altered SST gradients imposed here in  $2\text{CO}_2$  were also utilized in a newer version of the GISS GCMAM (Rind et al., 2002a). Its Hadley Cell response had certain similarities and some differences to the results presented here, a result as discussed in that paper that was influenced by the differences in physics parameterizations. Nevertheless, in comparison to a run with weaker SST gradients, its Hadley Cell was still amplified during Dec-Feb.

Doubled  $\text{CO}_2$  simulations by other modeling groups often show an increase in Hadley Cell intensity, although the specific characteristics of the changes differ greatly. For example, Watterson et al. (1995) using the CSIRO GCM found the Hadley Cell shifted upwards associated with increased latent heat release (similar to the results shown for the doubled  $\text{CO}_2$  experiments in Figure 4), and there was also a poleward shift in the regions of tropical ascent. In contrast, Dettinger et al. (see footnote 1) using the PCM model found an equatorward shift in the region of ascent, with poleward shifts in the region of descent. Douville et al (2002) with the CNRM GCM and Thompson and Pollard (1995) with the GENESIS model found an intensified Hadley circulation, although in the latter study that occurred only with a penetrating convection scheme. Ramstein et al. (1998) found that the LMD model simulated a 10% reduction in intensity for doubled  $\text{CO}_2$ . None of these authors clearly relate the results to the pattern of sea surface temperature changes, in particular to the magnitude of tropical warming, a feature which differs strongly from model to model (Rind, 1987) and so may be an influencing factor in model differences.

A more direct comparison can be made with the results of Magnusdottir (2001). Using the CCM3 model, the SST gradient was changed so that it was increased from  $10^\circ\text{S}$  to about  $12^\circ\text{N}$ , and then decreased to  $30^\circ\text{N}$ . The Hadley Cell response in Dec-Feb mimicked the gradient change: increased intensity from  $5^\circ\text{S}$  to  $10^\circ\text{N}$ , and decreased  $10$ - $30^\circ\text{N}$ . The results were reversed when these gradient changes were reversed. The gradient changes used were those estimated from annual average changes between 1903-1994; they have the same pattern over the tropical region as the  $2\text{CO}_2$  results (see Rind et al 2002b, Figure 1) and produced a Hadley Cell response qualitatively similar to that shown in Figure 4a. Our GCM experiments show that the precise patterns of SST change, including the small (latitudinal average) peaks in SST, have a dominant influence on the (modeled) Hadley Cell especially in Dec-Feb, qualitatively similar to the response of axisymmetric models (Schneider and Lindzen, 1977; Schneider, 1977; Lindzen and Hou, 1988).

### *B. Budget implications*

As discussed in the introduction, Pfeffer (1981) and others have used the budget terms to imply causality, however, equation (2), whether for the current climate or climate change situation, simply implies equivalence. The results for the different climates represent the equilibrium response of the model (or the observations) consistent with the climatological streamfunction, arrived at theoretically via interaction with the “forcing” terms. To the extent that any streamfunction change does not in itself alter the forcing terms, the distinction would be minimal. For example, the equilibrium radiative budget for a 2% solar irradiance increase would show no net imbalance, as the outgoing longwave radiation would have adjusted to the temperature increase, but it would still indicate a 2% increase in solar irradiance impinging upon the upper atmosphere. How important, then are the Hadley Cell changes for the individual budget terms?

Hadley Cell changes can influence the magnitude of  $dQ/dy$  by altering the vertical motion field, affecting convective heat release, although in these experiments they cannot alter the sea surface temperature gradients, which are specified. The sea surface temperature gradients are strongly associated with the resulting Hadley Cell changes, implying that they are forcing the Hadley Cell response in these experiments. In the real world, for both current and paleoclimates, the boundary forcing terms would be interactive with the Hadley Cell, especially at low and subtropical latitudes.

Similarly, subsidence in the subtropics can warm the atmosphere in that region, amplifying the latitudinal temperature gradient across mid-latitudes and influencing baroclinic instability and eddy forcing. While the Hadley Cell change can therefore affect the eddies, in these experiments there are very strong changes in the extratropical latitudinal temperature gradient (driven by the specified SSTs and radiative forcing) and topography from the different climate regimes which will likely have a much stronger impact on the eddies. In this sense the eddy changes are more like the +2% solar irradiance forcing in the example given above, relatively independent of the streamfunction response, and so more closely represent true “eddy forcing”. Hence the different budget terms will have a varying degree of interaction with the streamfunction changes.

As implied by the correlations, the diabatic forcing term is driven by the gradient in precipitation largely via the latent heat of condensation associated primarily with moist convection. Radiation (shortwave plus longwave) aids the circulation (i.e.,  $dQ/dy$ ) but is much less important in the equilibrium calculation. However, as noted by Betts and Ridgway (1988), longwave radiative cooling drives subsidence, which brings dry air down to the boundary layer and is associated with subtropical evaporation, the moisture source for the latent heat release that drives the circulation. A crude calculation, using the approach of Betts and Ridgway (1988), shows that the increased outgoing longwave radiation in the subtropics in the standard Paleocene simulation (due to the warmer temperatures) results in increased subsidence and hence increased latent heat flux, on the order of 70% of the observed change. For the ice age, with decreased outgoing longwave radiation, the reduced subsidence would have led to about 50% of the observed latent heat flux decrease. Given that the outgoing radiation change is due to the altered temperatures, which are themselves influenced by the change in condensation and thus latent heat fluxes, this is another example of the interdependence of various forcing terms. Ultimately, of course, radiation differences drive the SST gradients and their changes in the different climate regimes, and the Hadley Cell differences.

The sensible heat flux term is proportional to the gradient between the ground and surface air temperatures. Processes which act to warm the atmosphere minimize this flux; hence the sensible heating term in equilibrium works against the condensation term (note in Fig. 5 bottom, the contribution to reducing the Hadley Cell from the sensible heating term near the equator).

What about the suggested importance of eddy heat fluxes to the intensity of the Hadley Cell? The total eddy forcing does affect the model's Hadley Cell intensity (Fig. 7). This is composed of 4 terms as is apparent from the definitions of L and G (equation 3), involving the convergences of the horizontal and vertical transports of heat and momentum. In both hemispheres, the modeled eddy horizontal heat transport is somewhat more important than the eddy horizontal momentum transport to the total eddy forcing of the Hadley Cell, while both vertical transport terms are even less important. This is true both for the control run itself, and for the change between climate experiments. Note that the effect of the model's coarse resolution might influence this result. The contribution of the stationary eddies to the horizontal heat transport varies with climate; in the subtropics during the Last Glacial Maximum, the stationary eddy forcing was more than 50% of the eddy heat transport effect, while the contribution was negligible in the Paleocene (with little topography and stationary wave energy). As a result of this eddy forcing, the Hadley Cell intensity does correlate significantly with transient eddy energy (Table 3) (in general agreement with the analysis of Trenberth and Stepaniak (2003), see footnote 1). In both solstice seasons, the eddy forcing of the Hadley Cell maximizes poleward of the diabatic source, and is more important for the off-equatorial intensity, a result also seen, to a lesser extent, in the analysis of Pfeffer (1981).

The nonlinear terms augment the Hadley Circulation intensity in the lower and upper troposphere, once the circulation is developed. This too is the result of two terms, with the advective thermal flux amplifying the Hadley Cell at low levels, and the advection of momentum providing amplification in the lower and especially the upper troposphere. This occurs in the climate change experiments as well, and in all cases the terms appear to act as positive feedbacks, strengthening the circulations. Similarly, Schneider (1977) calculated that inclusion of the nonlinear advection of momentum by the mean circulation amplified its components in the upper and lower troposphere.

The diabatic forcing, the nonlinear flux response, and the eddy forcing help in generating the Ferrel Circulation (Figs. 5-9). Offhand, one would suppose that with a stronger Ferrel Cell, the Hadley Cell extent would be reduced. Nevertheless, there is no correlation between transient eddy energy and Hadley Cell poleward extent. One reason is that the eddies are generating a stronger subtropical portion of the Hadley Cell at the same time that they generate the Ferrel Cell, as can be seen in the figures; the effects then nullify one another.

The different experiments have greatly different topography, which could influence the Hadley Cell extent through its effects on both standing wave energy and the mountain torque. However, the correlation between standing wave energy and extent is not significant due to the existence of other forcing factors. The mountain torque in the control run acts to extend the Hadley Cell (Fig. 5a, bottom), and its lack in the Paleocene therefore helps limit the extent (Fig. 8, bottom). As noted in Table 2, the Paleocene has the most equatorward extent, and as can be seen from Figure 8, all of the terms contribute to this result.

During the Ice Ages, the increase in topography is at fairly high latitude, and as big high pressure systems build over the ice sheets, it is largely within an east wind regime. The increased mountain torque thus acts to limit the Hadley Cell extent at lower mid-latitudes, while inducing a negative contribution to the streamfunction further poleward. As a secondary effect to the mountain wave drag, this helps to extend the vertically-integrated streamfunction poleward.

#### *C. Hadley Cell changes and soil moisture*

A prime reason for understanding Hadley Cell sensitivity is to gauge how soil moisture changes with climate, given that the current regions of Hadley Cell descent are arid, while Hadley Cell ascent regions are moist. As shown in Table 3, both the Hadley Cell intensity and extent are related to precipitation gradients. However, Hadley cell changes are not a perfect predictor of soil moisture, which is the variable whose effect is most likely observed in paleoclimate studies, and is of most importance for societal impacts. We correlated the precipitation changes during the two solstice seasons with the actual soil moisture changes among the simulations; the results are given in Table 4. In about half the cases the correlation was significant at the 95% level. Overall, the latitudinal-average precipitation change accounts for about 40% of the variance in soil moisture in the two solstice seasons in the different experiments. Soil moisture is affected by evaporation changes as well, a function of the temperature and humidity, and so during the ice age, a precipitation decrease does not necessarily mean a soil moisture reduction. Also, the soil moisture values in individual seasons are affected by precipitation/soil moisture changes in other seasons. Given that the Hadley Cell changes themselves do not account for all the precipitation differences, the results suggest that the importance of Hadley Cell changes for paleo-moisture variations, while significant, do not account for a majority of the soil moisture variability in the model.

#### *D. Longitudinal variations*

In this section we discuss a number of issues related to longitudinal variations, which can affect the Hadley Cell and the interpretation of its change in the paleo data. An overall question concerns the relative importance of zonally-averaged circulation changes like the Hadley Cell to the actual site-specific results found by paleoclimate researchers. How much of what is seen locally in climate change scenarios is the result of an organized, latitudinal response to large-scale patterns, and how much is determined locally by particulars of geography, nearby ocean currents, etc.? This is an unanswerable question in general; Lonnie Thompson (see footnote 1) showed some ice age results from 6 geographically spaced tropical ice cores that indicated a general concurrence in response, therefore appearing to represent a true Hadley Cell change. The reality is obviously that any particular observational site will represent a mixture of large and small-scale phenomena, and only multiple sites covering a wide range of longitudes will allow for generalization related to the Hadley Cell.

Conversely, when the Hadley Cell changes, how representative is that of the change at any particular longitude? We can assess the longitudinal variance in meridional cell response by comparing the changes in upwelling in the tropics. Shown in Figure 11 are the results for the Dec-Feb time series of the different sets of runs. When the Hadley Cell changes are strong (as in PALEOCENE, or 2CO<sub>2</sub>-A) most of the longitudes have a similar response. When the changes are smaller (e.g., the ice age runs) there is much greater inconsistency in longitudinal response. Thus even when the Hadley Cell change is

statistically significant, it may not have much bearing on the change in the meridional cell or its expected consequences at any particular longitude (location).

It can be seen in Figure 11 that there is considerable similarity in the longitudinal response in the two simulations for each of the different climates, and to the extent this is true, one cannot easily use longitudinal variations in paleo-data to “back out” the appropriate latitudinal variation in SST. Between the two doubled CO<sub>2</sub> simulations the longitudinal changes in tropical vertical motion correlate at 0.4 (98% significance), while for the two runs in the Paleocene, the correlation is 0.81 (>99%). Therefore even when the magnitude of the Hadley Cell change is very different due primarily to different latitudinal gradients in SSTs, the longitudinal variation in response has certain similarities, most likely driven by continental position, topography and perhaps a warming/cooling climate. Cook (2003) noted from GCM experiments that the presence of land with its increased surface friction intensified the Hadley circulation, presumably with preferred longitudinal locations for the direct cell. Nakamura (1978) noted that mountains shift the subtropical high and subtropical subsidence northward via their blocking effect on west winds, requiring geostrophic adjustment of the pressure field. The various angular momentum effects of the continental ice sheets during the LGM were discussed above. The different ice age and Paleocene experiments each have in common the differing land/topography variations from the current climate.

How important are longitudinal variations in SSTs to what happens to the Hadley Cell? Longitudinal circulation cells responding to such SST gradients could theoretically divert energy from meridional cells (e.g., during El Niños, both the Hadley Cell and Walker circulations are altered). All of the runs discussed differed in their longitudinal gradients across the ocean basins, in somewhat random ways (see Fig. 2). The impact on these circulations can be estimated from the tropical vertical motion changes in Figure 11; the Walker circulation changes, for example, can be estimated by comparing the results at 90°-120W with 140-170°E (140 to 170). With this as an index, compared to the control run for Dec-Feb, the two Paleocene simulations showed a decrease in the Walker circulation by 70-80%, ICE AGE had a decrease of 58%, and 2CO<sub>2</sub> a decrease of 15%. ICE AGE -A showed a small increase (9%) with little change in 2CO<sub>2</sub>-A. When these changes are compared to the Hadley Cell peak changes (Table 2) there is no apparent relationship.

A complicating factor in the real world is that the relationship is complex: currently the Hadley Cell intensity is increased during El Niño time periods (e.g., Fig. 1). But as discussed by Gagan and Thompson (this book), the response of the Hadley Cell to other forcings (such as the precession-cycle) can even force the ocean response in the opposite fashion (i.e., greater Hadley Cell due to the orbital forcing resulting in more La Niñas).

Finally, what about the longitudinal gradient changes between ocean basins, as might happen with a change in frequency in El Niño, or reduction in North Atlantic Deep Water production and associated ocean heat transports in the Atlantic? To better address this issue, we can use idealized experiments in which the latitudinal gradients in different ocean basins are altered one at a time, or increased in one ocean basin and decreased in another, setting up a change in the longitudinal gradients between the basins (Rind et al., 2001b). The response, compared to altering the gradients similarly in each basin was that there is now no relationship with the zonally averaged SST gradient. As discussed in

Rind et al. (2001b), when tropical temperatures warm in one ocean basin (i.e., Atlantic or Pacific) relative to the other, a longitudinal circulation cell is set up with relative rising air in the warmer basin and relative descent in the other. In the basin with relative descent, the Hadley Cell intensity also diminishes, as the tropical descent mitigates the normally rising air. The net effect is to make the zonally averaged circulation practically independent of the zonally averaged SST gradient. Given the width of the Pacific relative to the Atlantic, the strongest (zonally-averaged) Hadley Cell occurred with a decreased gradient (i.e., cooler tropics) in the Atlantic, which led to rising air in the Pacific and an overall amplification of the zonally averaged meridional circulation. The weakest Hadley Cell response came with an increased gradient in the Atlantic and decreased gradient in the Pacific, as both effects minimized the direct meridional circulation cell in the Pacific. With respect to a particular past or future climate scenario, it is clearly important to know how each of the major ocean basins is responding.

#### *E. Comparison with paleo-data*

The discussions given above obviously bear on any comparisons of the model Hadley Cell response with paleodata. If the variation in soil moisture in any given season is primarily affected by processes other than the latitudinal average precipitation, then Hadley Cell changes for individual seasons are not necessarily indicative of what appears in the paleorecord. With this major caveat, we note that for the LGM, in the model the Hadley Cell during Dec-Feb intensified and expanded with both sets of SSTs, while in June-Aug it weakened (strengthened) and expanded (little change) in IA (IA-A). Thompson et al. (see footnote 1) showed results from six different tropical/semitropical ice core locations, which implied a weakening of the Hadley Cell, a result not really obtained with either SST pattern used (except for June-Aug in IA with the CLIMAP data). Ramstein et al. (1998) with the LMD model and CLIMAP (1981) SSTs (hence like IA) also found the Hadley Cell intensified, only in their case it occurred especially in June-Aug (with a 20% increase).

Chylek et al. (2001) suggested that enhancement of dust source areas during past glacial periods implied a contraction of the Hadley Cell, inconsistent with IA and to some extent IA-A, although as noted in the Results section, the model effect was largely due to the inclusion of added mountain drag. Without the added drag, there was little change in latitudinal extent with either SSTs in Dec-Feb. Ramstein et al. (1998) also found that the Hadley Cell poleward limit expanded, by about 3° latitude, roughly similar to the values estimated here. To emphasize the model dependency of such specific results, we note that in a finer resolution GISS model (with a top at 10mb and hence no explicit gravity wave drag), the Ice Age Hadley Cell was slightly contracted (Rind, 1988). Koutavas and Lynch-Stieglitz (this volume) concluded that the equatorward extent of the Hadley Cell as indicated by the ITCZ location shifted southward during the Ice Ages, especially during June-August. This result occurred in the model only with the warmer tropical SSTs (IA) (Fig. 4b); during Dec-Feb it occurred with the cooler values (IA-A).

While there is little direct evidence of Hadley Cell changes in the PALEOCENE, Farrel (1990) has suggested that the more “equable” climates may well have had a more expanded Hadley Cell, allowing for the symmetric circulation to transfer energy to high latitudes. With both sets of SSTs, the model’s Hadley Cell for this time period contracted its poleward extent (Table 3 and Figure 4).

## V. CONCLUSIONS

There are many suppositions concerning how the Hadley Cell responds to climate changes, and the implications for the paleo/future climate of such responses. We explore the general rules governing Hadley Cell changes in the context of the various thermal and momentum forcing terms contributing to the mass streamfunction. We compare general circulation model experiments for the Paleocene (58 million years ago), the Last Glacial Maximum (21k BP) and the doubled CO<sub>2</sub> climate with respect to the current climate. In addition to the standard experiments, each simulation is also run with an altered prescription of sea surface temperatures incorporating a greater tropical sensitivity. Finally, we comment on what the Hadley Cell changes actually mean with respect to soil moisture variations that might appear in the paleo-record.

The primary results are given below.

*With respect to Hadley Cell intensity*

- There is little relationship between the intensity and the magnitude of the global or equatorial temperatures;
- The peak intensity is most strongly related to the gradients of SST between the tropics and subtropics, which affects the gradient of latent heat release;
- When the SST latitudinal gradient change differs strongly between ocean basins, the Hadley Cell is much less related to the overall gradient;
- Eddy forcing, particularly transient eddy transports of heat, affects the off-equatorial Hadley Cell intensity;
- There is no significant correlation between the Hadley Cell intensity in the two winter hemispheres.

*With respect to Hadley Cell extent:*

- The Hadley Cell poleward extent is also not simply related to the mean temperature, being affected by numerous processes including those associated with the altered topography in these experiments;
- In particular, the extent is not strongly correlated with the equator-to-pole temperature gradient, as has been postulated from simple axisymmetric models.

*With respect to paleoclimate interpretations:*

- When the Hadley Cell changes are strong, there is good coherence between the sense of the local meridional circulation change (at any particular longitude) and the overall response;
- In experiments with weaker, though still significant changes, there is much variation in longitudinal response, making the Hadley Cell a poor interpreter of local paleo-data;
- The Hadley Cell change, while significantly correlated with seasonal soil moisture changes over land, does not account for a majority of the model's percentage changes due to conflicting influences of precipitation and temperature variations, and the influence of soil moisture changes in preceding seasons;
- The model results do not agree particularly well with the [rather?] uncertain paleoclimate interpretations of Hadley Cell change.

The various budget terms indicate all the processes that must be appropriately modeled for the Hadley Cell and its change to be successfully simulated. A number of these processes are affected by the SST boundary conditions and topography, thus uncertainties in these input fields will affect the results. As shown here, uncertainties especially in the tropical SSTs can produce larger Hadley cell differences for a particular climate than occur between climate regimes (e.g., the ICE AGES during JUNE-AUGUST, the PALEOCENE during DEC-FEB). The relevant processes are also affected by model parameterizations and resolution, so the different results obtained with different models are not surprising, although there may well be several common denominators in model simulations: the relationship of Hadley Cell intensity to the SST gradient between the tropics and subtropics, especially in Dec-Feb, and the influence of the monsoon, especially in June-August. Comparison with paleodata interpretations of Hadley Cell response is complicated by the uncertain influence of Hadley Cell changes on local field data. Understanding the Hadley Cell response in past climates, and using it to “back-out” the tropical sensitivity remains a challenging problem, as is predicting the future response of Hadley Cell changes and their climatic implications.

#### ACKNOWLEDGMENTS

We thank Patrick Lonergan for help in obtaining climate model diagnostics and figure preparation. Climate modeling at GISS is supported by the NASA Climate Program Office, while the development and use of the stratospheric model for climate change experiments is funded by the NASA ACPMAP program.

#### APPENDIX

$\bar{u}$  latitudinal average zonal wind

$\bar{v}$  latitudinal average meridional wind

$\bar{\omega}$  latitudinal average vertical wind in pressure coordinates

$\bar{\psi}$  mass streamfunction in pressure coordinates

$f$  coriolis parameter

$S_p, \sigma$  static stability parameters in pressure coordinates

$\bar{L}$  zonal average eddy momentum flux divergence

$\bar{G}$  zonal average eddy heat flux divergence

$\bar{F}$  zonal average friction

$\bar{Q}$  zonal average heating

#### REFERENCES

- Becker, E. and G. Schmitz, 2001: Interaction between extratropical stationary waves and the zonal mean circulation. *J. Atm. Sci.*, **58**, 462-480.
- Betts, A. K. and W. Ridgway, 1988: Coupling of the radiative, convective and surface fluxes over the equatorial Pacific. *J. Atm. Sci.*, **45**, 522-536.

- Chylek, P., L. Lseins, and U. Lohmann, 2001: Enhancement of dust source area during past glacial periods due to changes of the Hadley circulation. *J. Geophys. Res.*, **106**, 18477-18485.
- CLIMAP Project Members, 1981: Seasonal reconstructions of the Earth's surface at the last glacial maximum. *Geol. Soc. Amer.*, Map and Chart Series, MC-36.
- Cook, K. H., 2003: Role of continents in driving the Hadley Cells. *J. Atmos. Sci.*, **60**, 957-976.
- Dima, I. M. and J. M. Wallace, 2003: On the seasonality of the Hadley Cell. *J. Atm. Sci.*, **60**, 1522-1527.
- Douville, H., F. Chauvin, S. Planton, J.-F. Royer, D. Salas-Melia and S. Tyteca, 2002: Sensitivity of the hydrological cycle to increasing amounts of greenhouse gases and aerosols. *Climate Dynamics*, **20**, 45-68.
- Fang, M. and K. K. Tung, 1997: The dependence of the Hadley circulation on the thermal relaxation time. *J. Atmos. Sci.*, **54**, 1379-1384.
- Fang, M. and K. K. Tung, 1999: Time-dependent non-linear Hadley circulation. *J. Atmos. Sci.*, **56**, 1797-1807.
- Farrell, B. F., 1990: Equable climate dynamics. *J. Atm. Sci.*, **47**, 2986-2995.
- Gagan, M. K. and L. G. Thompson, 2004: Evolution of the Indo-Pacific warm pool and Hadley-Walker circulation since the last deglaciation. [This volume].
- Hansen, J., G. Russell, D. Rind, P. Stone, A. Lacis, S. Lebedeff, R. Ruedy and L. Travis, 1983: Efficient three dimensional global models for climate studies: models I and II. *Mon. Wea. Rev.* **111**, 609-662.
- Held, I. M. and A. Y. Hou, 1980: Nonlinear axially symmetric circulations in a nearly inviscid atmosphere. *J. Atmos. Sci.* **37**, 515-533.
- IPCC, 2001: *Climate Change 2001. The Scientific Basis*. Summary for Policymakers and Technical Summary of the Working Group I Report. 98 pp., Cambridge university Press, United Kingdom.
- Kim, H. K. and S. Lee, 2001: Hadley cell dynamics in a primitive equation model. Part II: Nonaxisymmetric flow. *J. Atm. Sci.*, **58**, 2859-2871.
- Koutavas, A. and J. Lynch-Stieglitz, 2004: Variability of the marine ITCZ over the eastern Pacific during the past 30,000 years: Regional perspective and global context. [This volume].
- Lindzen, R. S. and A. Y. Hou, 1988: Hadley circulations for zonally-averaged heating centered off the equator. *J. Atmos. Sci.*, **45**, 2416-2427.
- Magnusdottir, G., 2001: The modeled response of the mean winter circulation to zonally averaged SST trends. *J. Climate*, **14**, 4166-4190.
- Nakamura, M., 1978: Dynamic effects of mountains on the general circulation of the atmosphere: IV. Effects on the general circulation of the baroclinic atmosphere. *J. Met. Soc. Japan*, **56**, 353-366.
- O'Connell, S., M. A. Chandler, and R. Ruedy, 1996: Implications for the creation of warm saline deep water: Late Paleocene reconstructions and global climate model simulations. *GSA Bulletin* **108**, 270-284.
- Oort, A. H. and J. J. Yienger, 1996: Observed interannual variability in the Hadley circulation and its connection to ENSO. *J. Climate*, **9**, 2751-2767.
- Pfeffer, R. L., 1981: Wave-mean flow interactions in the atmosphere. *J. Atm. Sci.*, **38**, 1340-1359.

- Pierrehumbert, R. T., 1995: Thermostats, radiator fins, and the local runaway greenhouse. *J. Atmos. Sci.* **52**, 1784-1806.
- Polvani, L. M. and A. H. Sobel, 2002: The Hadley circulation and the weak temperature gradient approximation. *J. Atmos. Sci.*, **59**, 1744-1752.
- Ramstein, G., Y. Serafini-Le Treut, J. Le Treut, M. Forichon, and S. Joussaume, 1998: Cloud processes associated with past and future climate changes, *Clim. Dyn.*, **14**, 233-247.
- Rind, D. and W. Rossow, 1984: The effects of physical processes on the Hadley circulation. *J. Atmos. Sci.* **41**, 479-507.
- Rind, D., and D. Peteet, 1985: LGM terrestrial evidence and CLIMAP SSTs: are they consistent? *Quaternary Research* **24**, 1-22.
- Rind, D., R. Suozzo, N.K. Balachandran, A. Lacis and G. L. Russell, 1988: The GISS Global Climate/Middle Atmosphere Model Part I: Model structure and climatology. *J. Atmos. Sci.*, **45**, 329-370.
- Rind, D., R. Suozzo and N.K. Balachandran, and M. Prather, 1990: Climate change and the Middle Atmosphere. Part 1. The doubled CO<sub>2</sub> climate. *J. Atm. Sci.*, **47**, 475-494.
- Rind, D., 1987: The doubled CO<sub>2</sub> climate: impact of the sea surface temperature gradient. *J. Atmos. Sci.* **44**, 3235-3268.
- Rind, 1988: Dependence of warm and cold climate depiction on climate model resolution. *J. Climate*, **10**, 965-997.
- Rind, D., 1998: Latitudinal temperature gradient and climate change. *J. Geophys. Res.*, **103**, 5943-5971.
- Rind, D., 2000: Relating paleoclimate data and past temperature gradients: some suggestive rules. *Quaternary Science Rev.*, **19**, 382-390.
- Rind, D., J. Lerner and C. McLinden, 2001a: Changes of tracer distributions in the doubled CO<sub>2</sub> climate. *J. Geophys. Res.* **106**, 28061-28079.
- Rind, D., P. Lonergan, J. Lerner and M. Chandler, 2001b: Climate change in the Middle Atmosphere: Part V: The paleostratosphere in warm and cold climates. *J. Geophys. Res.* **106**, 20195-20212.
- Rind, D., J. Perlwitz, J. Lerner, C. McLinden and M. Prather, 2002a: The Sensitivity of tracer transports and stratospheric ozone to sea surface temperature patterns in the doubled CO<sub>2</sub> climate. *J. Geophys. Res.* **107**, DOI10.1029/2002JD002483
- Rind, D., P. Lonergan, N. K. Balachandran, and D. Shindell 2002b: 2xCO<sub>2</sub> and solar variability influences on the troposphere through wave-mean flow interactions. *J. Meteor. Soc. Japan.* **80**, 863-876.
- Schneider, E. K. and R. S. Lindzen, 1977: Axially symmetric steady-state models of the basic state for instability and climate studies. Part I: Linearized calculations. *J. Atmos. Sci.* **34**, 263-279.
- Schneider, E.K., 1977: Axially symmetric steady-state models of the basic state for instability and climate studies. Part II: Nonlinear calculations. *J. Atmos. Sci.* **34**, 280-296.
- Sobel, A. H., and C. S. Bretherton, 2000: Modeling tropical precipitation in a single column. *J. Climate.*, **13**, 4378-4392.
- Taylor, K. E., 1980: The roles of mean meridional motions and large-scale eddies in

- zonally averaged circulations. *J. Atmos. Sci.* **37**, 1-19.
- Thompson, S. L. and D. Pollard, 1995: A global climate model (GENESIS) with a land-surface transfer scheme (LSX). Part II: CO<sub>2</sub> sensitivity. *J. Climate*, **8**, 1104-1121.
- Trenberth, K.E. and D. P. Stepaniak, 2003: Seamless poleward atmospheric energy transports and implications for the Hadley circulation. *J. Climate*, **16**, 3705-3721.
- Trenberth, K.E., D. P. Stepaniak, and J.M. Caron, 2000: The global monsoon as seen through the divergent atmospheric circulation. *J. Climate*, **13**, 3969-3993.
- Waliser, D. E., Z. Shi, J. R. Lanzante, and A. H. Oort, 1999: The Hadley circulation: assessing NCEP/NCAR reanalysis and sparse in-situ estimates. *Climate Dyn.*, **15**, 719-735.
- Watterson, I. G., M. R. Dix, H. B. Gordon and J. L. McGregor, 1995: The CSIRO nine-level atmospheric general circulation model and its equilibrium present and doubled CO<sub>2</sub> climates. *Aust. Met. Mag.*, **44**, 111-125.
- Webb, R.S., S.J. Lehman, D. Rind, R. Healy and D. Sigman, 1997: Influence of ocean heat transport on the climate of the Last Glacial Maximum. *Nature*, **385**, 695-699.

Table 1. Primary experiments used.

EXPERIMENT	DESCRIPTION	REFERENCE
CONTROL	Current sea surface temperatures (SSTs)	Rind et al., 1988
2CO <sub>2</sub>	Doubled atmospheric CO <sub>2</sub> , GISS calculated SSTs with significant tropical warming	Rind et al., 1990
2CO <sub>2</sub> -A	Doubled atmospheric CO <sub>2</sub> , GFDL-like SSTs with minimal tropical warming	Rind et al., 1990
IA	Last Glacial Maximum with CLIMAP SSTs	CLIMAP, 1981; Rind et al., 2001
IA-A	Last Glacial Maximum with colder tropical SSTs	Webb et al., 1997; Rind et al., 2001
PAL	Paleocene (58MYa) with doubled atmospheric CO <sub>2</sub> , "best guess" SSTs	O'Connell et al., 1996; Rind et al., 2001
PAL-A	Paleocene with doubled atmospheric CO <sub>2</sub> with GISS 2xCO <sub>2</sub> SSTs	Rind et al., 2001

Table 2. Characteristic changes in the climate experiments.

	$\Delta$ HADLEY CELL PEAK (%)		$\Delta$ POLEWARD EXTENT (°)		$\Delta$ GLOBAL SURF TEMP (°C)		$\Delta$ EQUAT. SST (°C)		$\Delta$ TRANSIENT EKE (%)	
	D-F	J-A	D-F	J-A	D-F	J-A	D-F	J-A	D-F	J-A
2CO <sub>2</sub>	-2.4	-23.9	0.5	-3.9	4.36	4.19	3.50	3.58	-6.2	-6.4
2CO <sub>2</sub> -A	-18.8	-13.5	1.4	1.3	4.29	4.38	1.54	1.54	-12.4	-16.1
IA	10.1	-23.3	4.3	0.7	-4.12	-4.45	-0.50	-1.95	55.1	30.6
IA-A	9.4	67.5	5.6	0	-7.98	-10.3	-7.30	-7.70	52.9	59.4
PAL	49.2	16.0	-7	-9	4.09	2.60	1.50	0.45	52.2	21.1
PAL-A	-11.7	-25.8	-0.1	-2	8.60	6.58	5.55	5.42	18.8	9.0

Table 3. Correlation of Hadley Cell characteristics and climate parameters.

	INTENSITY		POLEWARD EXTENT	
	NH, DEC-FEB	SH, JUN-AUG	NH, DEC-FEB	SH, JUN-AUG
Surf. Temp.	-0.20	<b>-0.73</b>	-0.65	-0.35
Equat. SST	-0.23	<b>-0.83</b>	-0.54	-0.28
SST Grad. 4N-27N (D-F) 12N-27S(J-A)	<b>0.99</b>	<b>0.81</b>	-0.59	-0.44
Precip. Grad. 4N-27N (D-F) 12N-27S(J-A)	<b>0.90</b>	0.62	<b>-0.80</b>	<b>-0.73</b>
NH/SH	0.41	0.41	<b>0.86</b>	<b>0.86</b>
Intensity/ Extent	-0.56	-0.05	0.56	0.05
Eddy Kinetic Energy (eke)	0.46	<b>0.80</b>	0.21	0.43
Transient eke	<b>0.87</b>	<b>0.74</b>	0.28	0.01
Standing eke	-0.55	-0.07	0.47	0.54
N'ward trans. Static Energy by Eddies	0.50	0.64	0.20	0.11
Grav Wave Drag	0.14	-0.67	<b>0.82</b>	-0.47
Surf friction	0.28	-0.25	-0.54	0.63

Table 4. Correlation between latitudinal precipitation and soil moisture changes in each experiment. Significance level is in parenthesis.

	Dec-Feb	June-Aug
2CO <sub>2</sub>	0.79 (.001)	0.75 (.005)
2CO <sub>2</sub> -A	0.59 (.04)	0.33 (0.30)
IA	0.50 (.10)	-0.36 (.25)
IA-A	0.54 (.06)	0.41 (.18)
PAL	0.74 (.006)	0.80 (.001)
PAL-A	0.86 (.0003)	0.65 (.02)



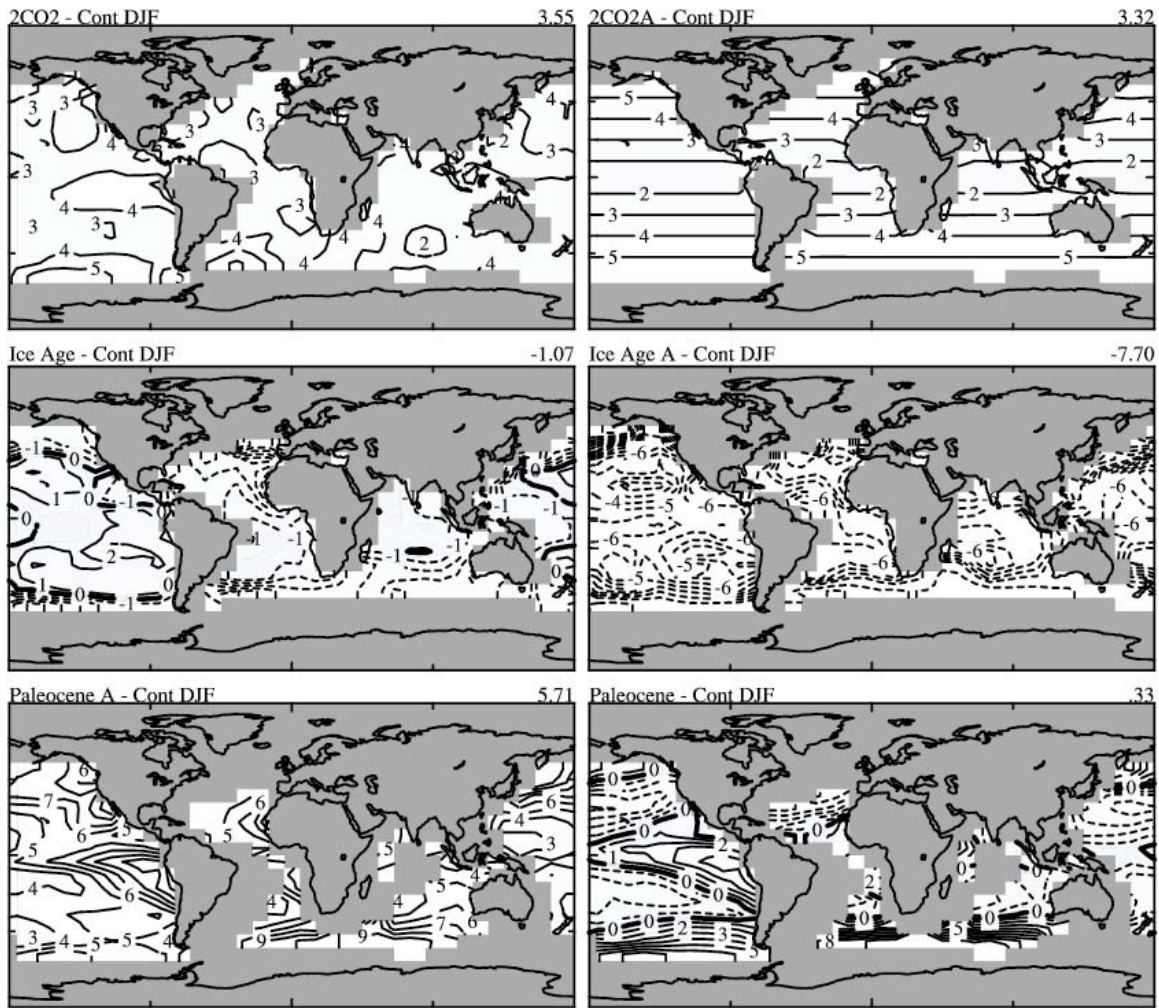


*Figure 2.* Change in sea surface temperatures relative to the control run for the different experiments. Sea ice regions are omitted. The altered land/ocean configuration in the Paleocene reduces the number of grid points that are also oceanic in the current climate.

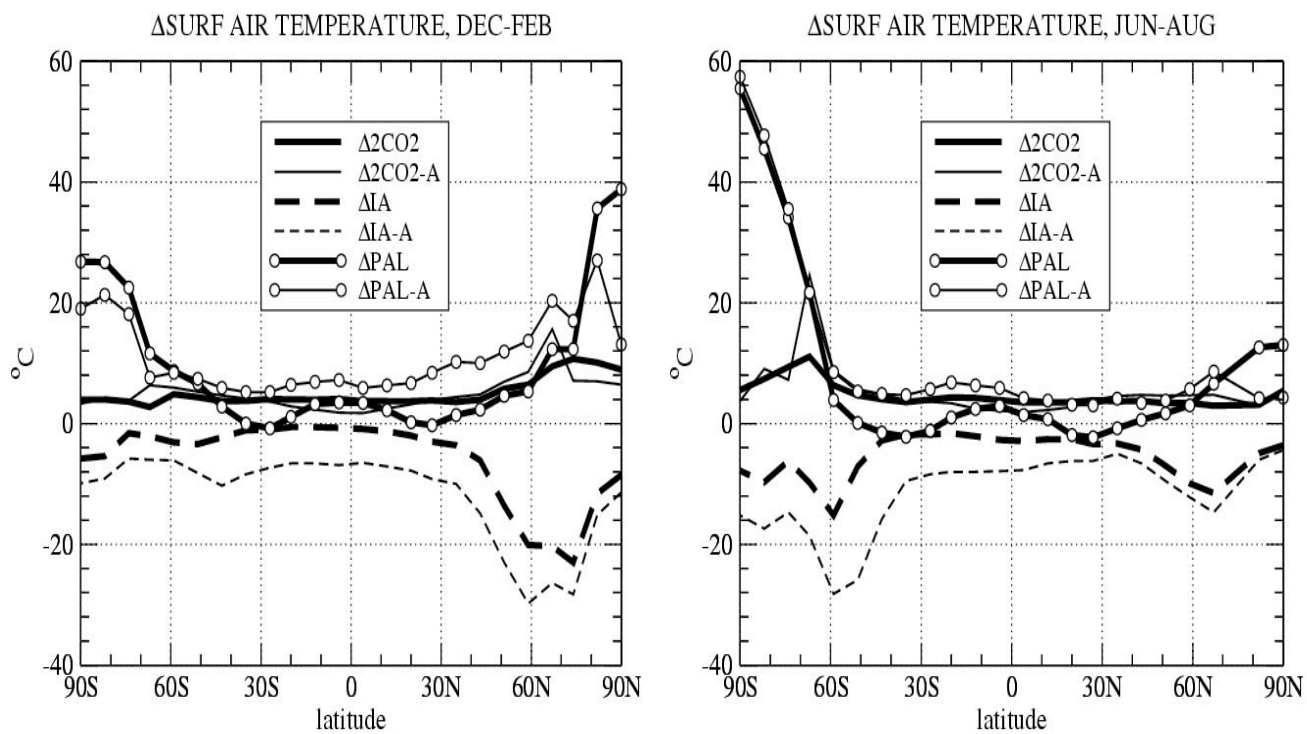


Figure 3. Zonal average surface air temperature changes in the two solstice seasons.

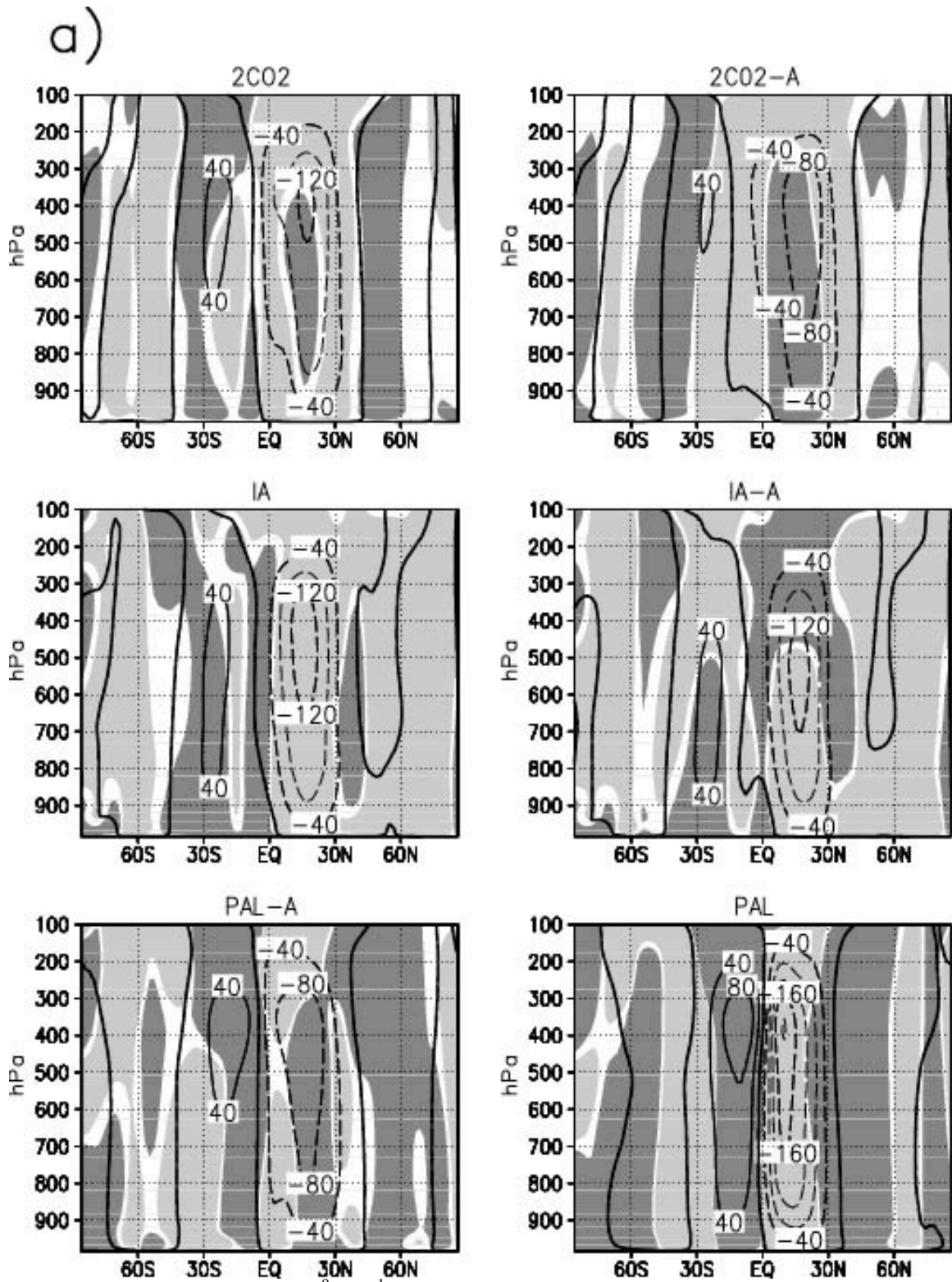


Figure 4. Streamfunctions ( $10^9 \text{ kg s}^{-1}$ ) for the two solstice seasons a) Dec-Feb and b) June-Aug. Light (dark) shading indicates where the negative (positive) changes between the experiment and the control are significant at the 95% level.

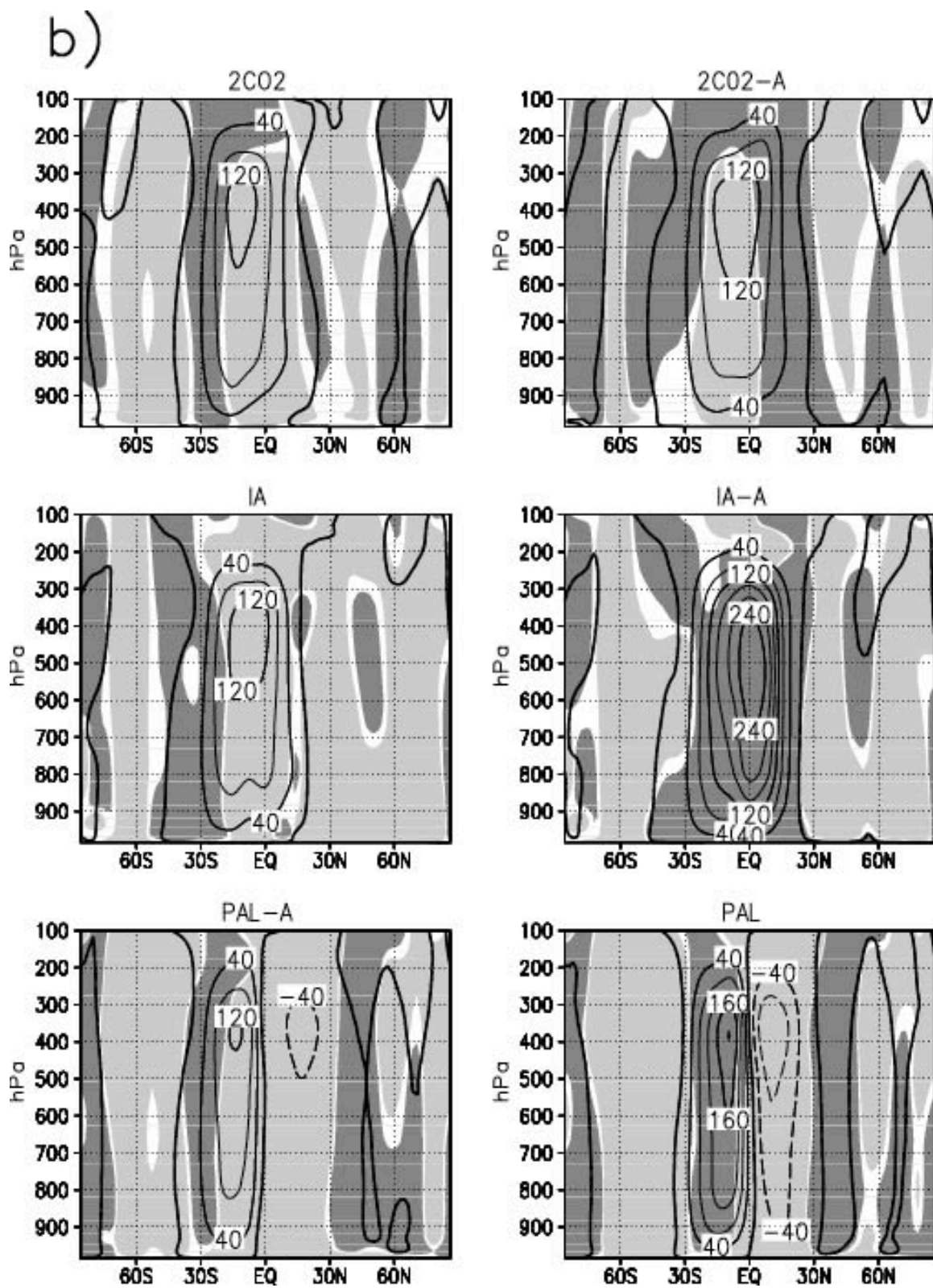


Figure 4. Continued.

## a) Control DJF

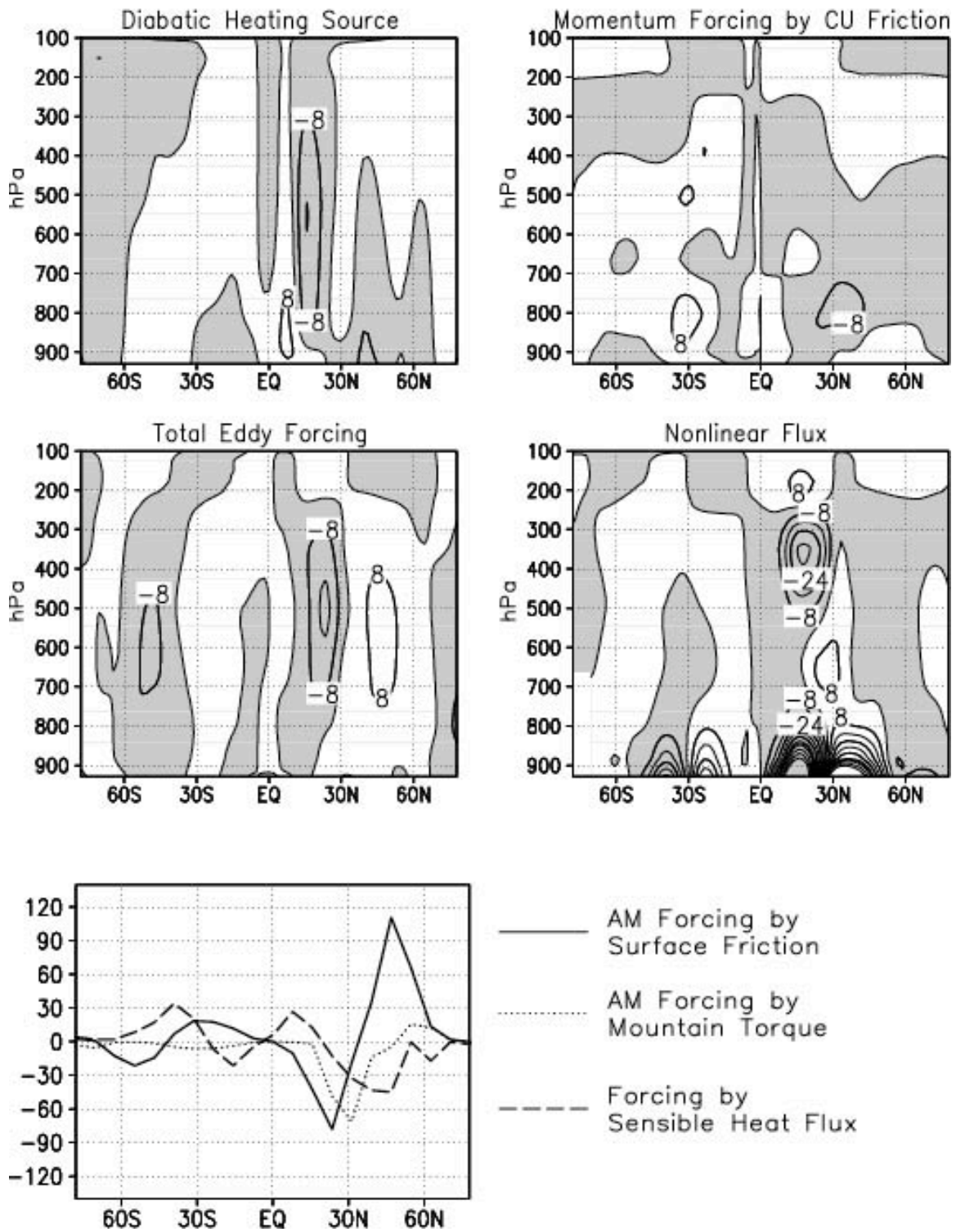


Figure 5. Contributions of individual terms ( $\text{W m}^2/\sigma$ ) to the Hadley Cell for the control run for (a) Dec-Feb and (b) Jun-Aug. Negative values are shaded.

## b) Control JJA

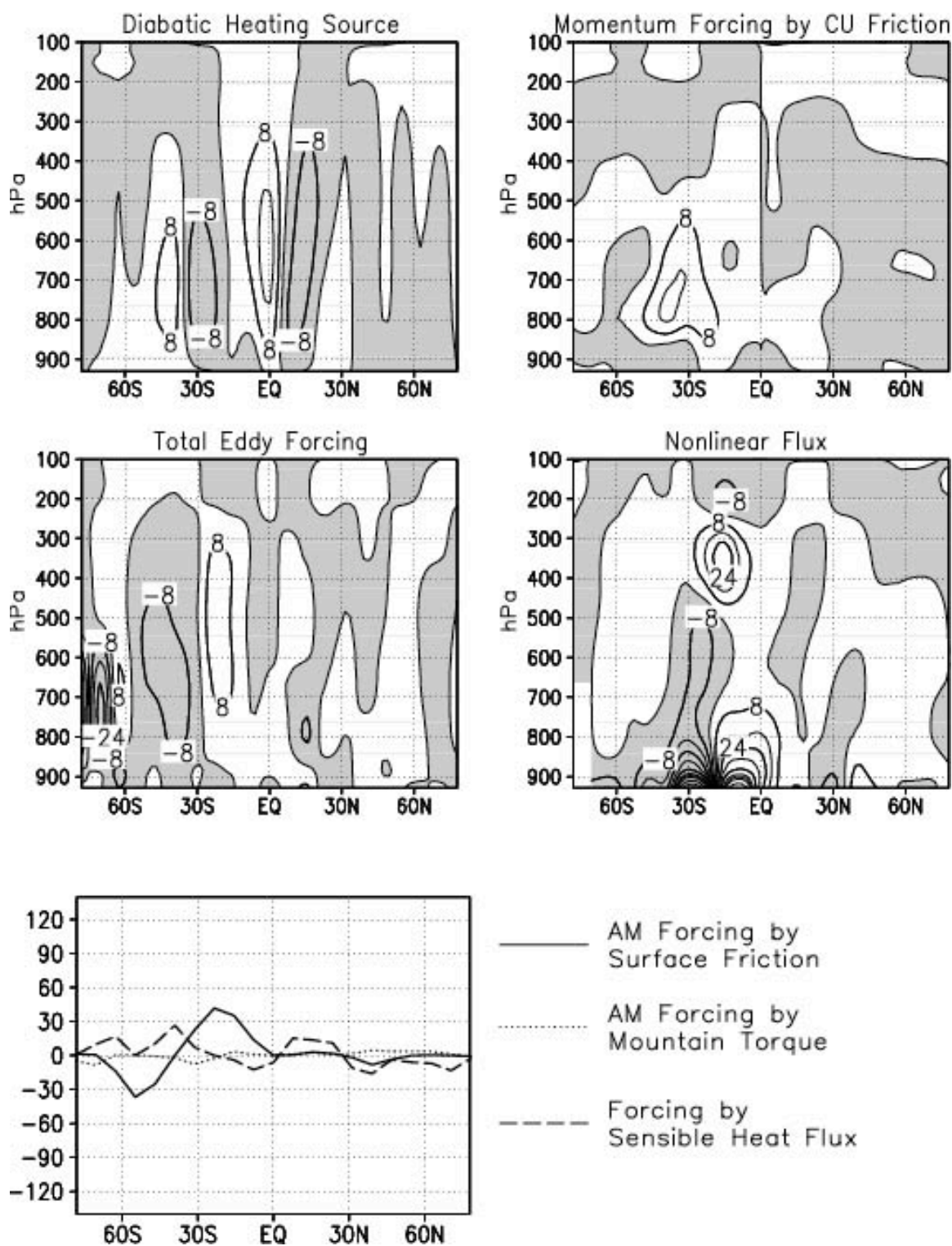


Figure 5. Continued.

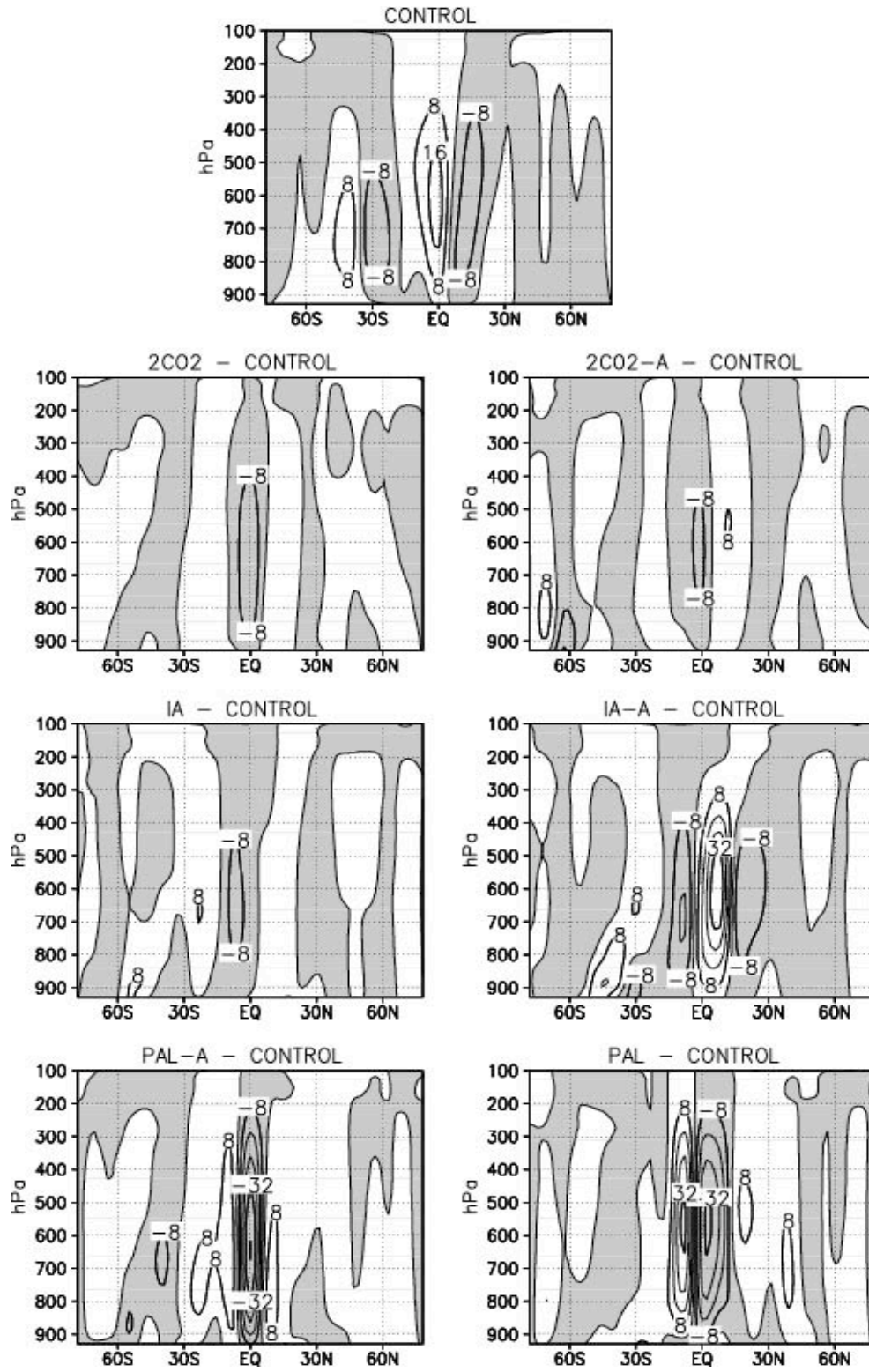


Figure 6. Change in diabatic heating source ( $\text{W m}^{-2}/\sigma$ ) for June-Aug. Negative values are shaded.

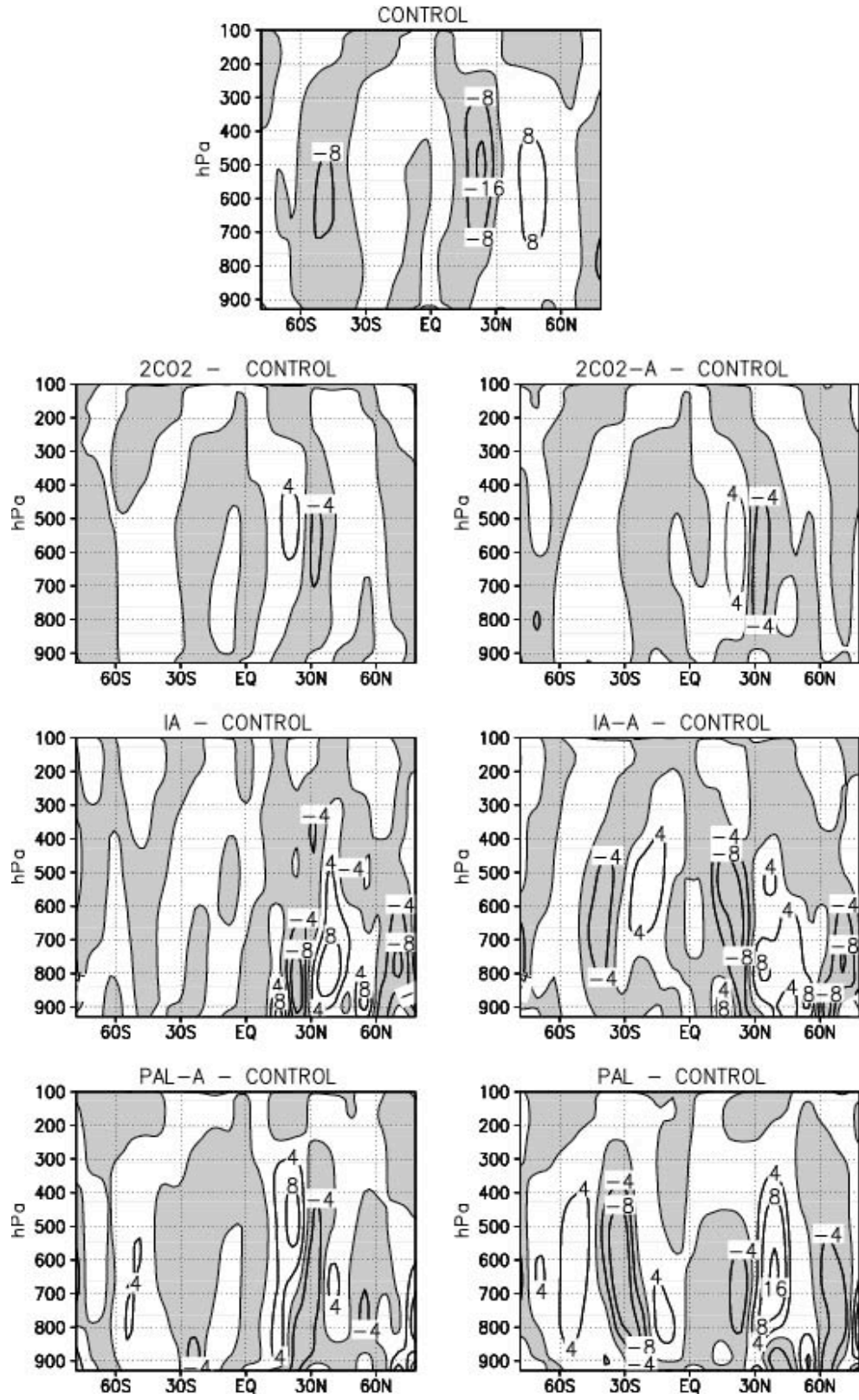


Figure 7. Change in total eddy forcing ( $\text{W m}^{-2}/\sigma$ ) for Dec-Feb. Negative values are shaded.

# PAL-CONTROL DJF

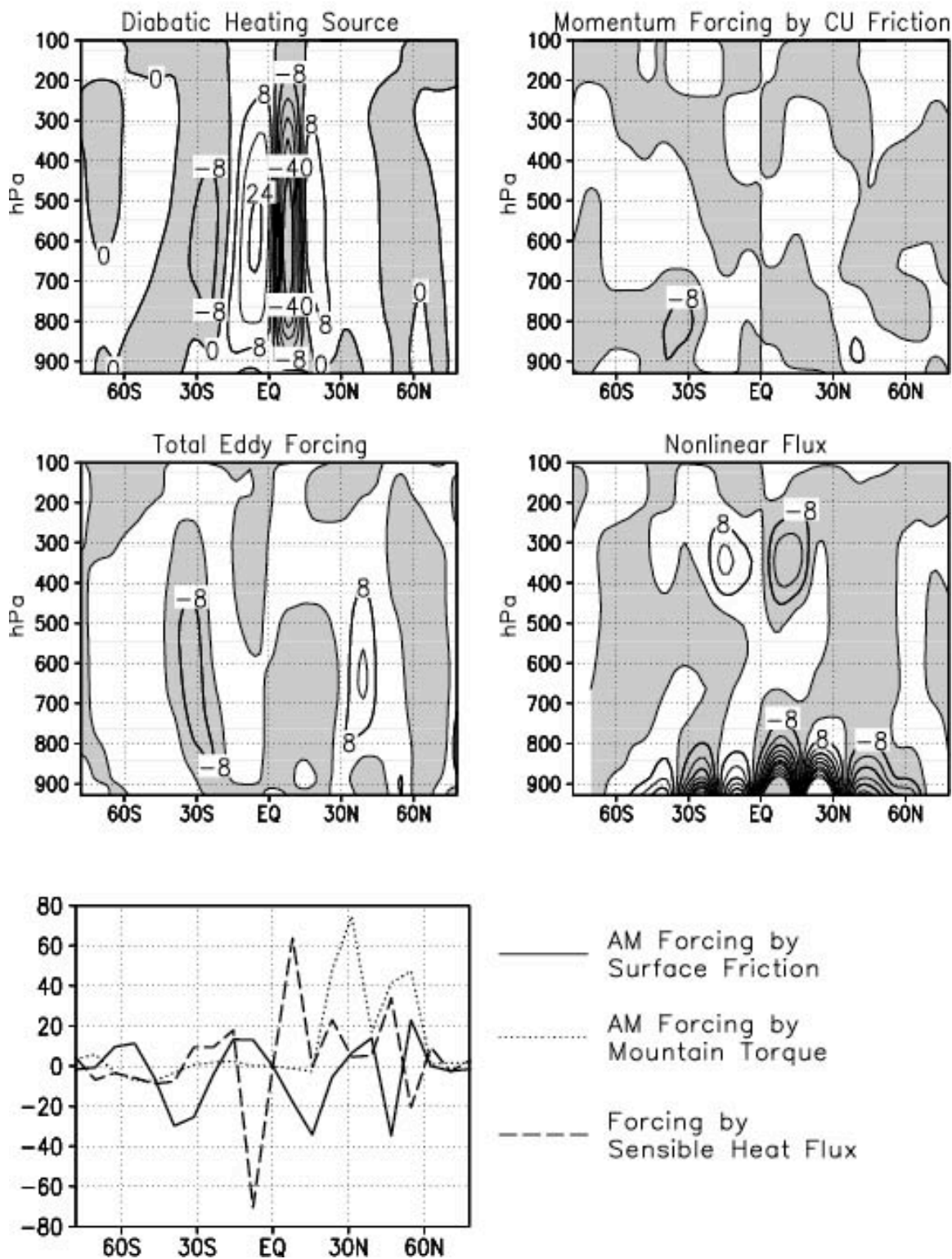


Figure 8. Contributions of the individual terms ( $\text{W m}^{-2}/\sigma$ ) in the Paleocene simulation for Dec-Feb. Negative values are shaded.

# IAa—CONTROL JJA

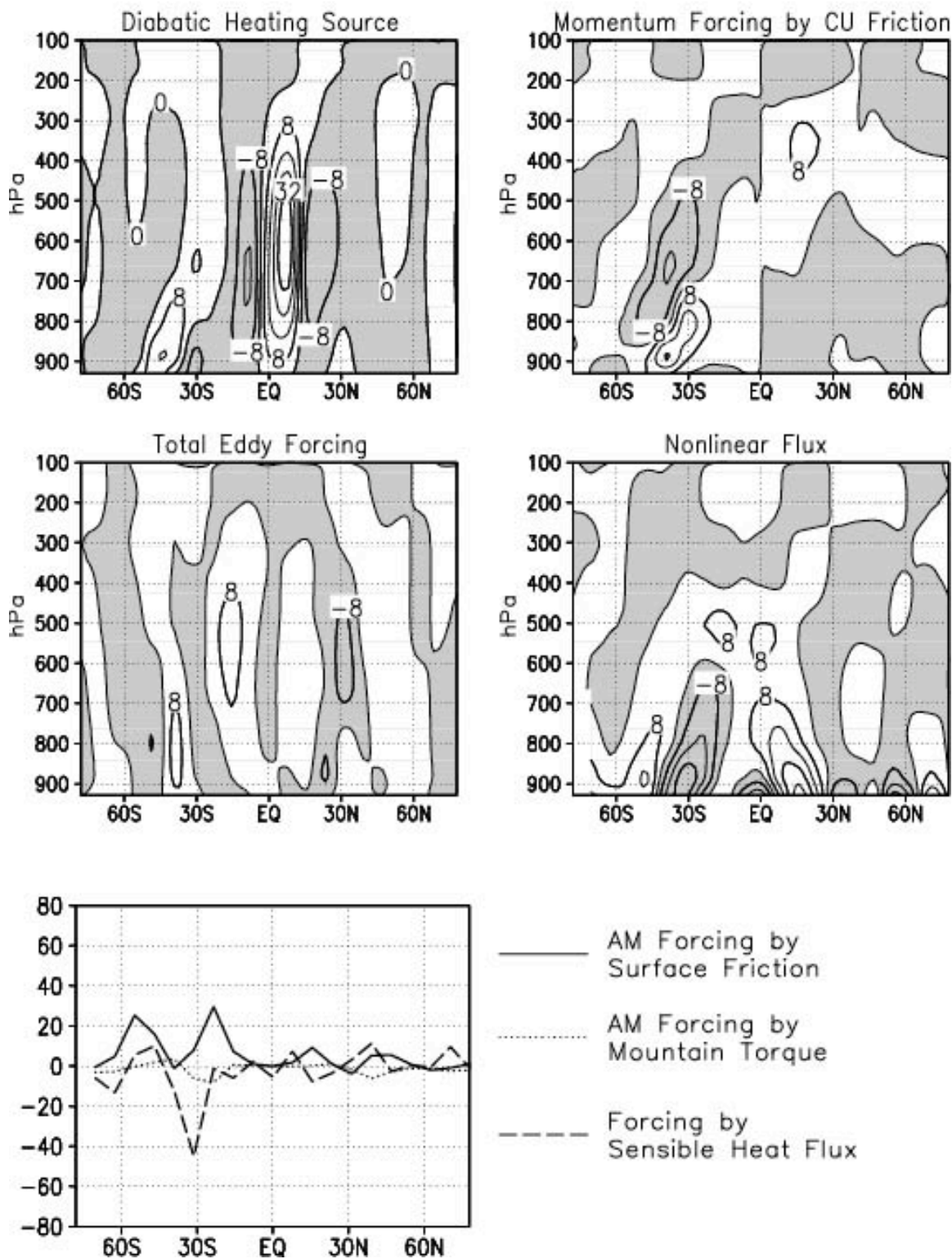


Figure 9. Contributions of the individual terms ( $\text{W m}^2/\sigma$ ) during the alternate Ice Age for June-Aug. Negative values are shaded.

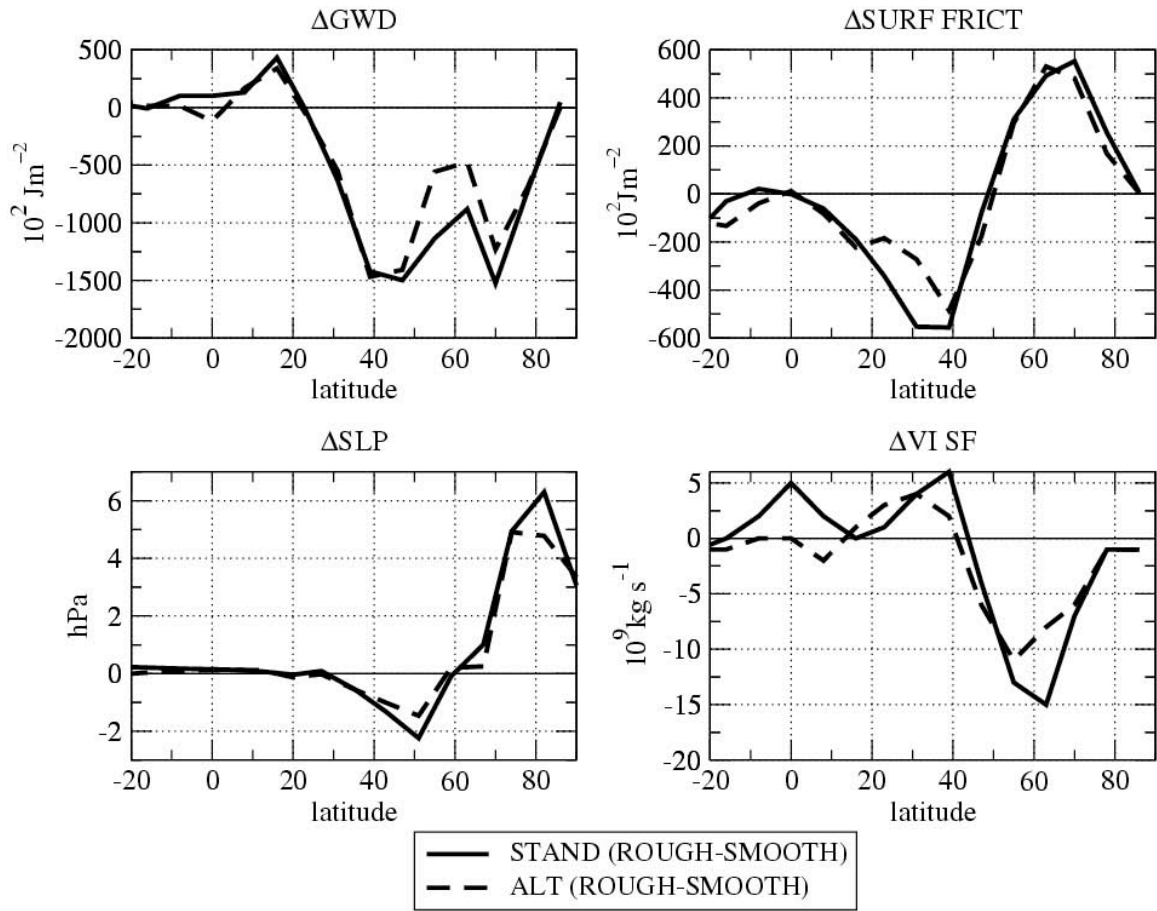


Figure 10. Differences between the rough ice sheet and smooth ice sheet ice age experiments for: the change of angular momentum by gravity wave drag (top left); change of angular momentum by surface friction (top right); sea level pressure (bottom left); vertically-integrated streamfunction (bottom right).

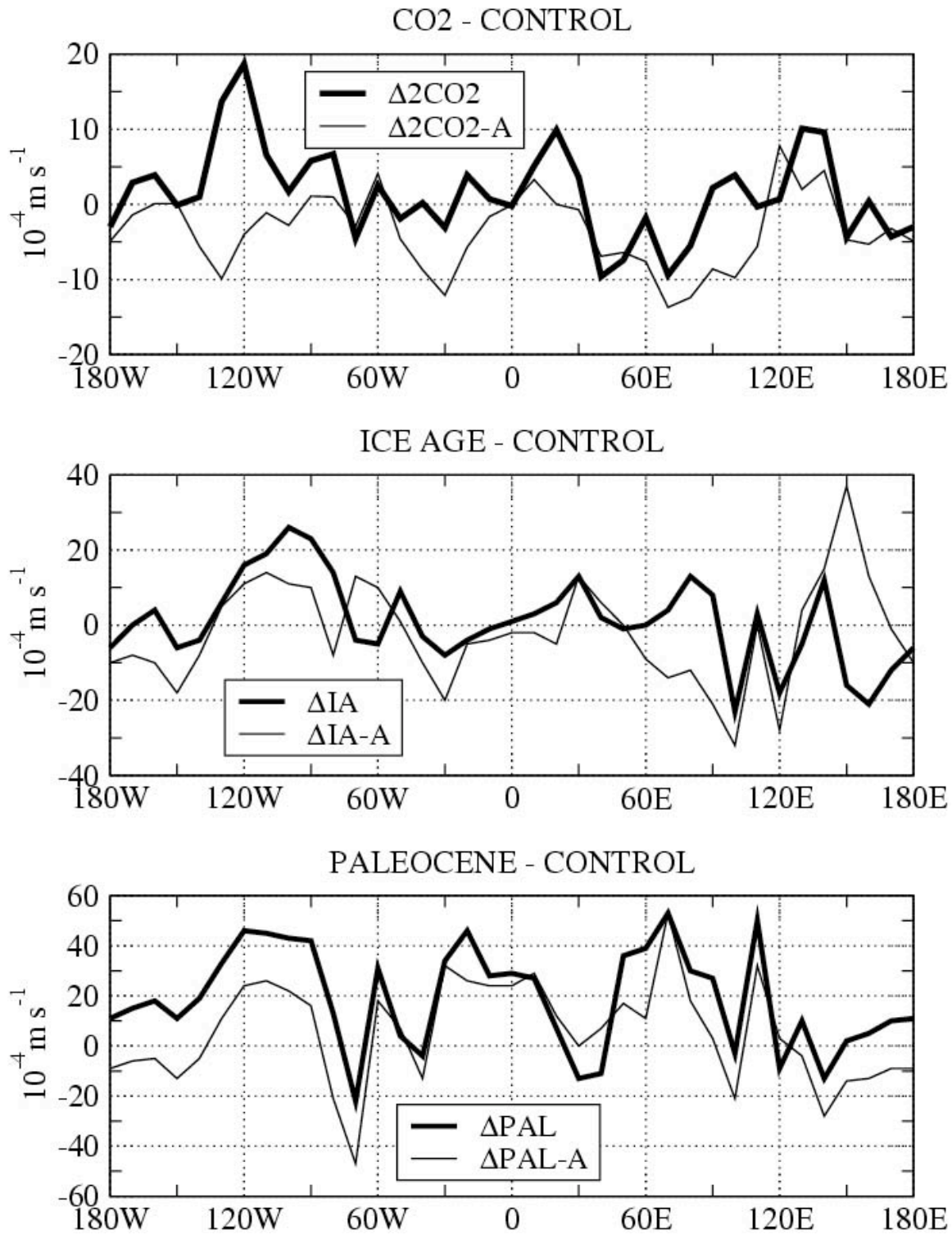


Figure 11. Change in tropical vertical velocity ( $8^{\circ}\text{N}$ - $16^{\circ}\text{S}$ ) in Dec-Feb in the different experiments relative to the control run. Shown are the runs for the two doubled  $\text{CO}_2$  experiments (top), ice age experiments (middle), and Paleocene runs (bottom).